Geol. Mag. **156** (*6*), *2019, pp. 950–968* © *Cambridge University Press 2018*
doi:10.1017/S0016756818000511

U–Pb ages and Hf isotopes of detrital zircons from pre-Devonian sequences along the southeast Yangtze: a link to the final assembly of East Gondwana

XIAO MA*‡, KUNGUANG YANG*‡† & ALI POLAT§¶

*School of Earth Sciences, China University of Geosciences, Wuhan 430074, China
‡Key Laboratory of Tectonics and Petroleum Resources, Ministry of Education, China University of Geosciences Wuhan, Wuhan 430074, China
§Department of Earth and Environmental Sciences, University of Windsor, Windsor, ON, Canada N9B 3P4
¶Center for Global Tectonics, School of Earth Sciences, China University of Geosciences, Wuhan 430074, China

(*Received* 6 April 2017; *accepted* 14 June 2018; *first published online* 22 August 2018)

Abstract – The Early Palaeozoic geology of the South China Craton (SCC) is characterized by an Early Palaeozoic intracontinental orogen with folded pre-Devonian strata and migmatites, MP/MT metamorphic rocks and Silurian post-orogenic peraluminous magmatic rocks in both the Yangtze and the Cathaysia blocks. In this contribution, we present new zircon U–Pb ages and Hf isotope data for detrital zircons from the Neoproterozoic to Silurian sedimentary sequences in the southeastern Yangtze Block. Samples from Neoproterozoic rocks generally display a major peak at 900–560 Ma, whereas samples from Lower Palaeozoic rocks are characterized by several broader peaks within the age ranges 600–410 Ma, 1100–780 Ma, 1.6–1.2 Ga and 2.8–2.5 Ga. Provenance analysis indicates that the 900–630 Ma detritus in Cryogenian to Ediacaran samples was derived from the Late Neoproterozoic igneous rocks in South China that acted as an internal source. The occurrence of 620–560 Ma detritus indicates the SE Yangtze was associated with Late Neoproterozoic arc volcanism along the north margin of East Gondwana. The change of provenance resulted in the deposition of 550–520 Ma and 1.1–0.9 Ga detrital zircons in the Cambrian–Ordovician sedimentary rocks. The εHf(*t*) values of these detrital zircons are similar to those of zircons from NW Australia–Antarctica and South India. This change of provenance in the Cambrian can be attributed to the intracontinental subduction between South China and South Qiangtang, and the convergence of India and Australia when East Gondwana finally amalgamated.

Keywords: South China, U–Pb dating, Hf isotope, Palaeozoic, Ediacaran, Gondwana, Detrital zircon

1. Introduction

The composite cratonic South China Craton (SCC) is one of the largest continental fragments in eastern Asia and consists of the Yangtze Block in the NW and the Cathaysia Block in the SE (Fig. 1). After the amalgamation of these two blocks during the Jiangnan Orogen at 1000–830 Ma (Wang *et al.* 2007; Zhao *et al.* 2011), the SCC was rifted in response to the break-up of Rodinia (Li *et al.* 1995; Li *et al.* 2002; Yu *et al.* 2008), and a Late Neoproterozoic basin, called the Nanhua basin (Wang & Li, 2003; Wang *et al.* 2015), formed as a failed rift basin in the craton. This basin was transformed into an orogeny in response to widespread Early Palaeozoic intracontinental orogenic events in southern China (Faure *et al.* 2009; Charvet *et al.* 2010; Wang *et al.* 2010*b*; Shu *et al.* 2014), which are assumed to have been associated with the final assembly of the supercontinent Gondwana during the Late Neoproterozoic to the Early Palaeozoic (Xu *et al.* 2014*a*, *b*).

Recently, a great deal of discussion has focused on Lower Palaeozoic successions of the SCC and their detrital zircon spectra, which indicate predominately Early Neoproterozoic and Latest Neoproterozoic to Early Cambrian sources (Wang *et al.* 2010*b*; Wu *et al.* 2010; Xu *et al.* 2012, 2013, 2014*a*, *b*; Li *et al.* 2013; Yao, Li & Li, 2014*a*; W. H. Yao *et al.* 2014*b*, 2015; Yu *et al.* 2014; Chen *et al.* 2016; Yao & Li, 2016). The ages of these zircons vary distinctly from those of the underlying Lower to Middle Neoproterozoic successions of the SCC (L. J. Wang *et al.* 2010, 2012; Hofmann *et al.* 2011; Wang & Zhou, 2012; W. Wang *et al.* 2013; Li, Li & Li, 2014), which lack Early Neoproterozoic detritus and are therefore interpreted to have been located far from the centre of Rodinia in the Neoproterozoic (Yu *et al.* 2008; Hofmann *et al.* 2011; Ma *et al.* 2016). In Early Palaeozoic reconstructions of Gondwana, the SCC has previously been proposed to be an isolated block separated from East Gondwana (Torsvik & Cocks, 2009) or adjacent to Laurentia (Wu *et al.* 2010; Li *et al.* 2013); however, the existence of similar Early Neoproterozoic and Latest Neoproterozoic to Early Cambrian detritus suggests a spatial link between the SCC and East Gondwana (Wang *et al.* 2010*b*; Xu *et al.* 2012, 2014*b*; Cawood *et al.* 2013; Yao *et al.* 2015; Yao & Li, 2016). Nevertheless, how and when these similar detritus grains were transported to the SCC remain unclear.

†Author for correspondence: yangkunguang@163.com

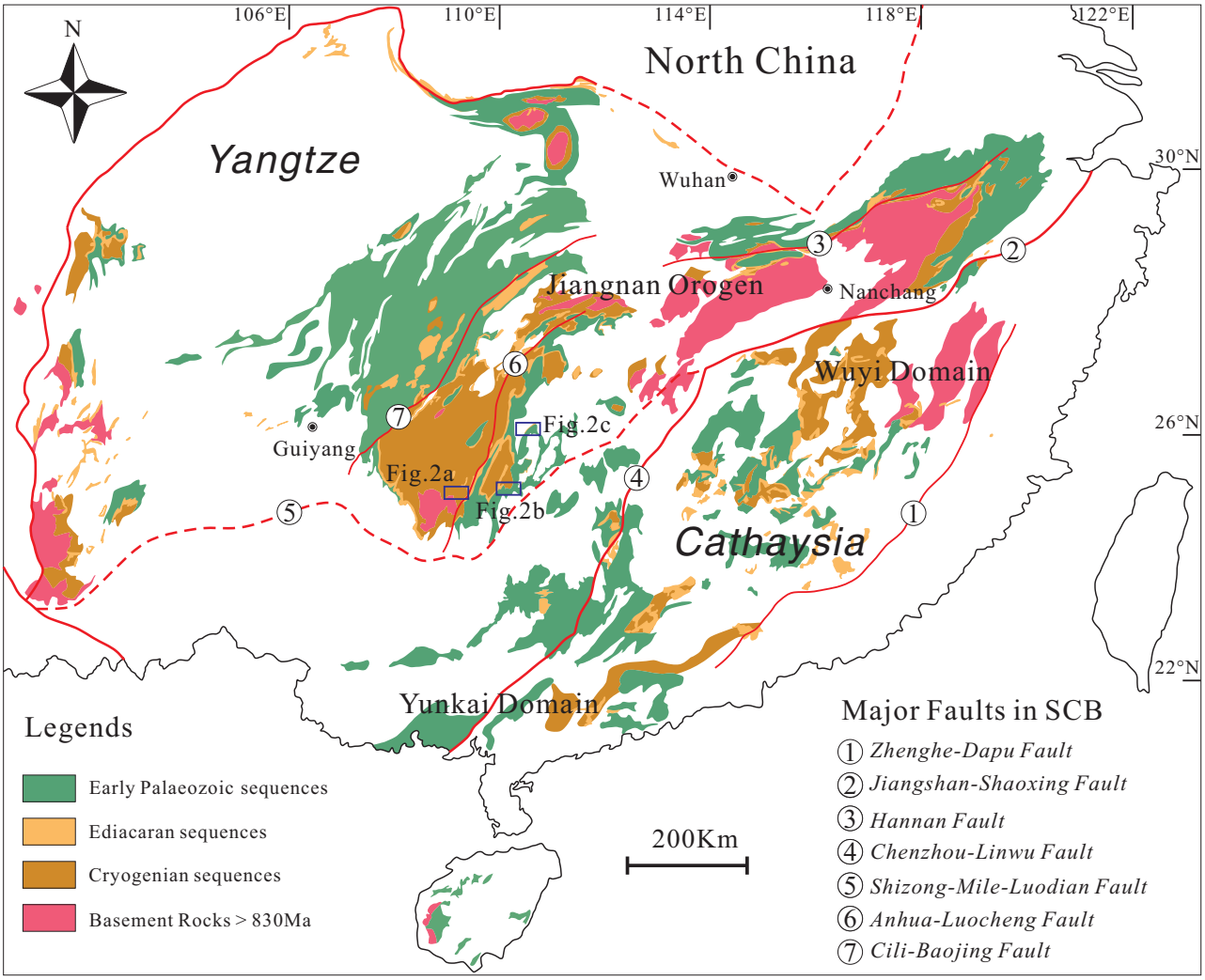

Figure 1. (Colour online) A simplified regional map highlighting the distribution of pre-Devonian sequences in South China.

The models that favour a SCC – East Gondwana link typically place the SCC among other Asian microcontinent fragments (such as Qiangtang, Lhasa, Sibumasu, Indo-China and Tarim) along the northern margin of East Gondwana in the Early Palaeozoic (Zhu *et al*. 2012; Hu *et al*. 2013, 2015; Y. J. Wang *et al*. 2013*b*; Burrett *et al*. 2014; Zhang *et al*. 2014). The details of the relative locations and tectonic settings of these continental fragments, however, remain controversial. One interpretation is that the northern margin of East Gondwana had a passive continental margin facing north during the Early Palaeozoic (Murphy & Nance, 1991; Miller *et al*. 2001), and that the regional unconformity between Ordovician and Cambrian strata resulted from extensional tectonic events after the Pan-African orogeny (Miller *et al*. 2001). Another school of thought is that the northern margin of East Gondwana was converted to an active continental margin in response to the final assembly of East Gondwana (Cawood, Johnson & Nemchin, 2007; Y. J. Wang *et al*. 2013*b*), which is defined by accretion (Cawood *et al*. 2017) or collision events (Yao *et al*. 2014*b*) between North India and South China during the Ediacaran and Cambrian.

In this contribution, we present new detrital zircon U–Pb ages and Hf isotopes from eight samples collected from the Upper Neoproterozoic to Silurian strata across the basin along the SE margin of the Yangtze. Based on these results, together with previously published detrital zircon data, we explore the potential sources for the sediments of the Upper Neoproterozoic to Silurian strata in the SE Yangtze to better address the provenance evolution of the SCC and its relationship with East Gondwana in the Early Palaeozoic.

2. Geological setting

The pre-Neoproterozoic crustal growth histories of the Yangtze and Cathaysia blocks of the SCC remained relatively different until their first amalgamation during the Neoproterozoic Jiangnan Orogeny (also called the Jinning Orogeny and the Sibao Orogeny by various authors, e.g. Zhao & Cawood, 1999, 2012; Wang *et al*. 2007; Li *et al*. 2009; Charvet, 2013). The pre-Neoproterozoic basement of the Yangtze Block is represented by (1) Archean rocks of the Kongling Complex in the northern part of the block (3.3–2.9 Ga

https://doi.org/10.1017/S0016756818000511 Published online by Cambridge University Press

and 2.1–1.8 Ga; Qiu *et al*. 2000; Zheng *et al*. 2006; Jiao *et al*. 2009; Gao *et al*. 2011) and (2) minor outcrops of 1.7–1.0 Ga metavolcanic and metasedimentary rocks along the SW margin of the block (Li *et al*. 2002; Greentree *et al*. 2006; Zhao *et al*. 2010), whereas that of the Cathaysia Block is characterized by (1) Upper Palaeoproterozoic (2.0–1.6 Ga) granites and granitic gneisses of the Badu, Chencai, Mayuan and Tianjingping complexes in the Wuyi area in the NE part of the block (Yu *et al*. 2009, 2012; Li *et al*. 2010) and (2) the *c*. 1.43 Ga Baoban Complex and the coeval Shilu Group metavolcaniclastic rocks of Hainan Island in the SW part of the block (Li *et al*. 2002, 2008).

The Neoproterozoic suture zone between the Yangtze and Cathaysia blocks is referred to as the Jiangnan Orogen, the Jiangnan Belt (Charvet *et al*. 1996) or the Jinning Belt (Faure *et al*. 2009). The *c*. 1500 km long suture zone is located near the present NE-trending Jiangshan–Shaoxing Fault (Fig. 1); however, the western extent of this belt remains uncertain. Voluminous Precambrian sedimentary strata and Neoproterozoic (1.0–0.7 Ga) igneous rocks are restricted to the area between the Cili–Baojing Fault and the Shizong–Mile–Luodian Fault (Fig. 1) (Zhao & Cawood, 2012; Cawood *et al*. 2013; Charvet, 2013; Y. J. Wang *et al*. 2013*a*), which is considered as the western extent of the Jiagnan Orogen in this contribution. The amalgamation of the Yangtze and Cathaysia blocks caused a rapid change in the tectonic setting, resulting in the formation of post-orogenic extensional basins and a depositional hiatus in South China. These processes are recorded by deposition of Upper Neoproterozoic rift sedimentary rocks that unconformably overlie the basement rocks (Du *et al*. 2013; Wang *et al*. 2015), and by contemporaneous mafic intrusions along the SE and NW margins of the Yangtze Block (Wang *et al*. 2008; Zhou, Wang & Qiu, 2009; Shu *et al*. 2011; Lin *et al*. 2016).

The Cambrian to Ordovician successions in Cathaysia feature typical slope and shallow-water facies with siliciclastic-dominated strata. These successions grade into carbonate-dominated strata in the Yangtze, which represent platform-type facies (Wang *et al*. 2010*b*; Xu *et al*. 2012; Shu *et al*. 2014, 2015; Yao, Li & Li, 2014*a*). In the Yunkai and Hainan domains of Cathaysia, the unconformity between the Cambrian and Ordovician strata was developed (termed the Yu'nanian Orogeny, e.g. Wang *et al*. 2010*b*; Xu *et al*. 2014*b*) and dies out to the north across the SCC where the Cambrian and Ordovician strata are conformable (BGMRGZP, 1987). In the Yunkai and Hainan domains, the Lower to Middle Cambrian both consist of interstratified quartz sandstone, mudstone, siltstone and phyllite (BGMRGXP, 1985; Xu *et al*. 2014*b*). The Upper Cambrian succession is absent. The Lower to Middle Cambrian successions are unconformably overlain by Lower Ordovician succession, which consist of conglomerate, sandy conglomerate and quartz sandstone (BGMRGXP, 1985).

The conformably overlying Silurian siliciclastic sedimentary rocks in Yangtze are absent across most of Cathaysia, and range in age from Lower Silurian in the SE Yangtze to Upper Silurian in the NW and NE Yangtze (Xu *et al*. 2012). From Cathaysia to the NW Yangtze, angular unconformities between the pre-Devonian and Upper Palaeozoic strata gradually change to disconformities, and mark the main phase of Early Palaeozoic orogeny in South China (Wang *et al*. 2010*b*; Y. J. Wang *et al*. 2013*a*).

3. Stratigraphic section and samples

Siliciclastic rock samples were systematically collected from the Upper Neoproterozoic to Silurian strata along the SE margin of the Yangtze (Fig. 1). Eight samples analysed for this study are from three sampling locations including the Congjiang area in the southeastern Guizhou province, the Longsheng area in the northwestern Guangxi province, and the Chengbu area in the southwestern Hunan province.

Two sandstone samples (QD53 and QD51) were collected from the Congjiang area in the southeastern Guizhou province, located to the west of the Anhua–Luocheng Fault and adjacent to the 835 Ma Yuanbaoshan granitic pluton (Fig. 2a). The Congjiang stratigraphic section consists of Upper Neoproterozoic (Cryogenian to Ediacaran) strata, comprising thick, locally micaceous, quartzite, chlorite–quartz–sericite phyllite, silty sericite phyllite, and mica schist (BRMRGZP, 1987; Ma *et al*. 2016).

Four sandstone samples (LS01, LS03, LS04 and LS07) were collected from the Longsheng area in the northwestern Guangxi province (Fig. 2b), located in the area to the east of the Anhua–Luocheng Fault. The Longsheng section consists of Ediacaran–Ordovician siliciclastic strata, comprising intercalations of shale, siltstone and sandstone (BGMRGXP, 1985), whereas the Silurian strata are absent and the Devonian conglomerate unconformably overlies the Ordovician strata.

Two sandstone samples (CB09 and CB10) were collected from the Chengbu area in the southwestern Hunan province (Fig. 2c), located to the east of the Anhua–Luocheng Fault and adjacent to the 430–400 Ma Miaoershan granitic pluton. The Chengbu section consists of Cambrian–Silurian strata, comprising the Cambrian–Ordovician siltstone and interlayered thin sandstone and Silurian fine-grained sandstones (BGMRHNP, 1988). The Silurian strata are intruded by the Miaoershan granite pluton, and both the pluton and the bedrocks are unconformably overlain by the Devonian conglomerate.

4. Analytical methods

4.a. Zircon separation and cathodoluminescence (CL) imaging

Zircons were separated using conventional heavy liquid and magnetic techniques. The zircons were then

https://doi.org/10.1017/S0016756818000511 Published online by Cambridge University Press

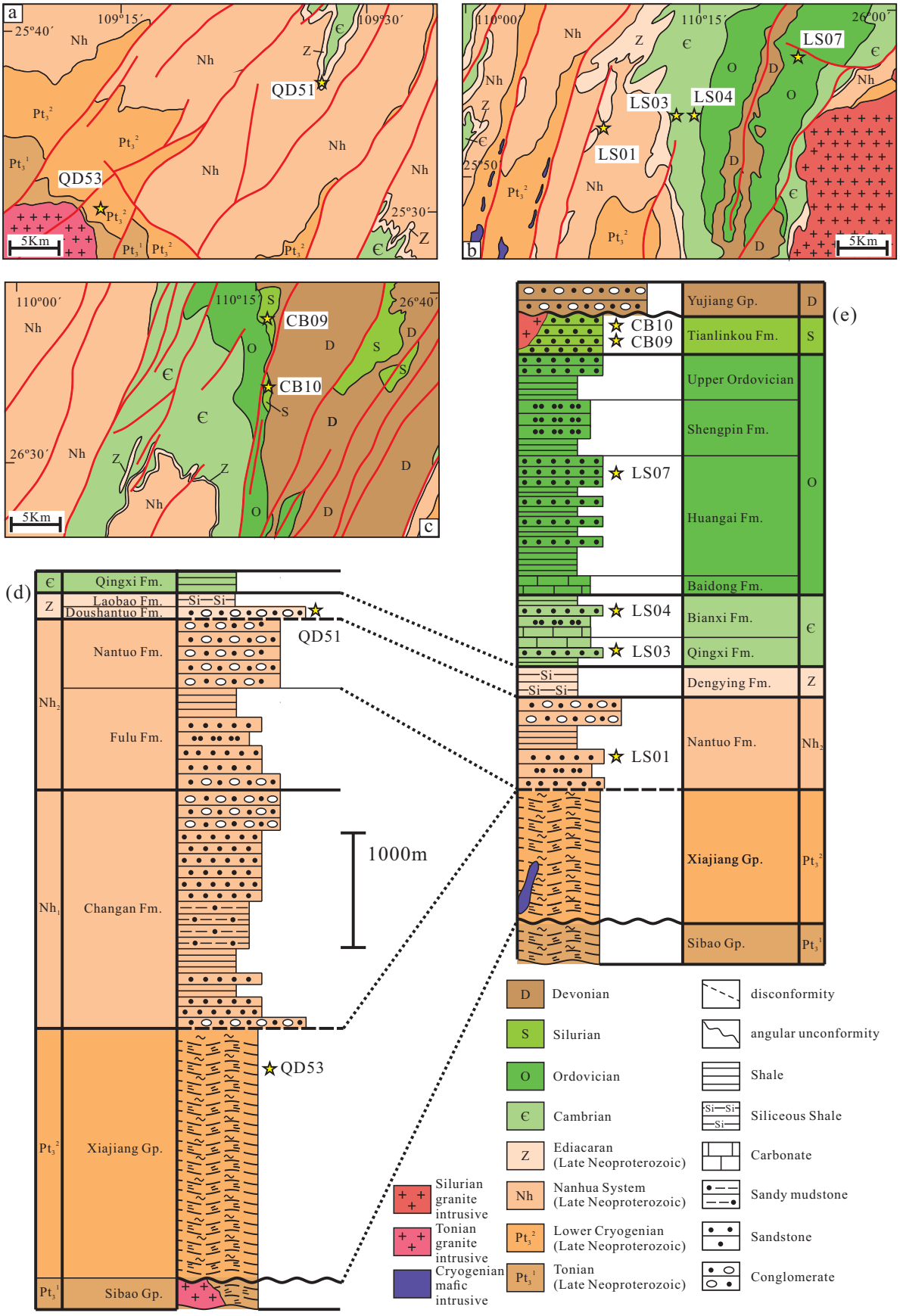

Figure 2. (Colour online) A regional geological map and sampling localities in the study area. (a) The Congjiang area in the southeastern Guizhou province; (b) the Longsheng area in the northwestern Guangxi Province; (c) the Chengbu area in the southwestern Hunan province; (d) the stratigraphy of the Congjiang area showing the sampling positions; and (e) the stratigraphy of the Longsheng and Chengbu area with sampling positions.

https://doi.org/10.1017/S0016756818000511 Published online by Cambridge University Press

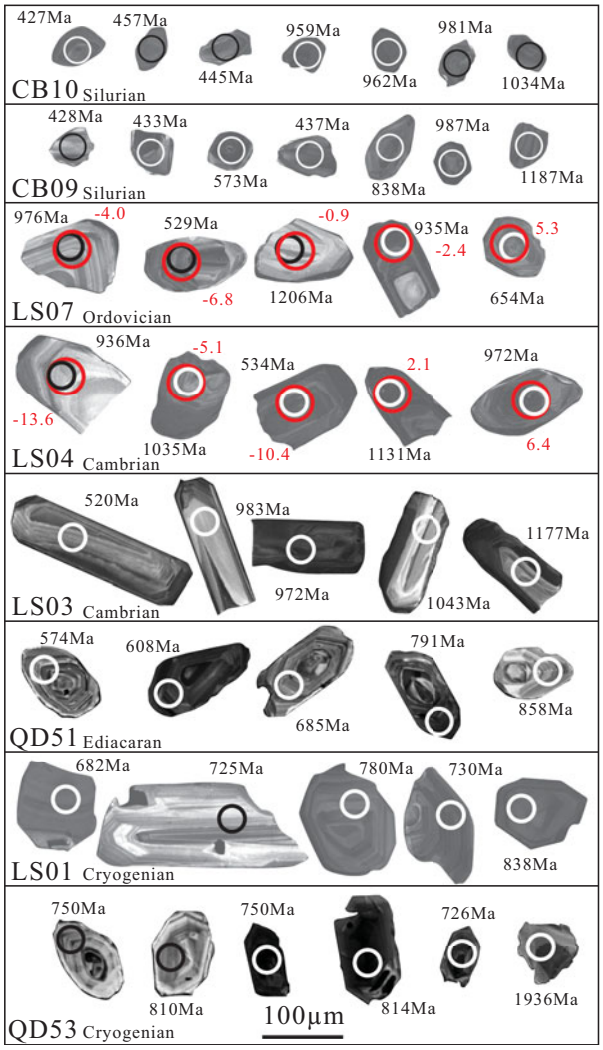

Figure 3. (Colour online) Cathodoluminescence (CL) images of the analysed zircon grains. The white or black circle represents the analytical plot on the zircon grain of LA-ICP-MS analysis, with the outer (red) circle representing the εHf(*t*) values.

purified by means of handpicking under a binocular microscope at the Langfang Regional Geophysical Survey, Hebei Province, China. Cathodoluminescence (CL) images were obtained using a JXA 8100 electron microprobe with a MonoCL3 system operated at 15 kV and 20 nA, at the State Key Laboratory of Geological Processes and Mineral Resources, China University of Geosciences (Wuhan). The CL images of representative zircons in this study are presented in Figure 3.

4.b. Zircon LA-ICP-MS U–Pb dating

The U–Pb dating of the zircons was conducted by LA-ICP-MS at the State Key Laboratory of Geological Processes and Mineral Resources, China University of Geosciences, Wuhan. The detailed operating conditions for the laser ablation system and ICP-MS instrument and the data reduction are given in Liu *et al.* (2008, 2010). A pulsed 193 nm ArF excimer laser at a repetition rate of 10 Hz was used for ablation. The energy density of laser ablation that was used in this study was 14 J cm^{-2}. The diameter of the analysis spot was 32 μm. An Agilent 7500a ICP-MS was used to measure the ion-signal intensity of the zircons. Helium was used as a carrier gas, and argon was used as the make-up gas and mixed with the carrier gas via a T-connector before entering the ICP. Nitrogen was added to the central gas flow (Ar + He) of the Ar plasma to enhance instrument sensitivity (Hu *et al.* 2008). Each analysis comprised a background acquisition of *c.* 20–30 s (gas blank) followed by 50 s of data acquisition from the sample. Each ablation was collected as an individual Agilent Chemstation file and processed offline. Offline selection of the background and analytic integrations, as well as instrument drift correction and quantitative calibration for the U–Pb dating, were performed using ICPMSDateCal (Liu *et al.* 2008, 2010). Zircon 91500 was used as external standard for U–Pb dating, and was analysed twice every five analyses. Time-dependent drifts of U–Th–Pb isotopic ratios were corrected using a linear interpolation (with time) for every five analyses according to the variations of 91500 (Liu *et al.* 2010). Uncertainty of preferred values for the external standard 91500 was propagated to the ultimate results of the samples. All of the U–Pb ages were calculated using the Isoplot 3.0 Excel macro of Ludwig (2003). All U–Pb ages are quoted at 1 sigma error with 90 % confidence level. Unless otherwise stated, the age data shown in the figures and in the discussions are $^{207}Pb/^{206}Pb$ ages for grains older than 1.0 Ga, and $^{206}Pb/^{238}U$ ages for grains younger than this age.

4.c. Zircon Lu–Hf isotopic analysis

The Lu–Hf isotopic analyses were conducted using a Neptune Plus MC-ICP-MS (Thermo Fisher Scientific, Germany) in combination with a Geolas 2005 excimer ArF laser ablation system (Lambda Physik, Göttingen, Germany) that is hosted at the State Key Laboratory of Geological Processes and Mineral Resources. The energy density of laser ablation used in this study was 5.3 J cm^{-2}. A 'wire' signal smoothing device is included in this laser ablation system, by which smooth signals are produced even at very low laser repetition rates down to 1 Hz (Hu *et al.* 2012*b*). More details on analytical and calibration procedures can be found in Hu *et al.* (2012*a*).

Interference of ^{176}Lu on ^{176}Hf was corrected by the directly obtained β_{Yb} value from the zircon sample itself in real time (Liu *et al.* 2010). The $^{179}Hf/^{177}Hf$ and $^{173}Yb/^{171}Yb$ ratios were normalized to $^{179}Hf/^{177}Hf = 0.7325$ and $^{173}Yb/^{171}Yb = 1.1248$ (Blichert-Toft, Chauvel & Albarède, 1997) using an exponential correction for mass bias. Interference of ^{176}Yb on ^{176}Hf was corrected by measuring the interference-free ^{173}Yb isotope and using $^{176}Yb/^{173}Yb = 0.7876$ (McCulloch, Rosman & De Laeter, 1977) to calculate $^{176}Yb/^{177}Hf$. Similarly, the relatively minor interference of ^{176}Lu on

https://doi.org/10.1017/S0016756818000511 Published online by Cambridge University Press

^{176}Hf was corrected by measuring the intensity of the interference-free ^{175}Lu isotope and using the recommended $^{176}Lu/^{175}Lu = 0.02656$ value (Blichert-Toft, Chauvel & Albarède, 1997) to calculate $^{176}Lu/^{177}Hf$ ratios. Offline selection and integration of analyte signals, and mass bias calibrations were performed using ICPMSDataCal (Liu *et al*. 2010).

5. Results

5.a. Zircon U–Pb ages

5.a.1. Sandstone samples from southeast Guizhou

All U–Pb analytical data are represented in Table S1 as online Supplementary Material at https://doi.org/10.1017/S0016756818000511. Sample QD53 was collected from the Upper Neoproterozoic Xiajiang Group (Cryogenian) sandstone layers in the Congjiang area in SE Guizhou (Fig. 2d). A total of 56 concordant (>90 %) ages ranging from 1936 to 693 Ma were obtained. Except for four pre-Neoproterozoic zircon ages at 1062 ± 83 Ma, 1220 ± 18.4 Ma, 1756 ± 18.9 Ma and 1936 ± 17.9 Ma, a single cluster at 890–693 Ma is dominant in the age spectrum.

Sample QD51 was collected from sandstones in the Upper Neoproterozoic Doushantuo Formation (Ediacaran) in the Congjiang area (Fig. 2d). A total of 37 concordant ages were obtained that are characterized mainly by 880–562 Ma ages with one age at 1482 Ma. Two main peaks occur at 610 Ma and 800 Ma.

5.a.2. Sandstone samples from northeast Guangxi

Sample LS01was collected from sandstones in the Upper Neoproterozoic Nantuo Formation (Cryogenian) in the Longsheng area (Fig. 2e). A total of 64 concordant ages were obtained (Fig. 4) that range from 2656 to 630 Ma. A predominating Neoproterozoic age range from 916 to 630 Ma makes up 73 % in all analyses in this sample, with a main peak at 790 Ma. Remaining analyses range from 2656 to 1915 Ma, with two sub-peaks at 2.0 Ga and 2.6 Ga.

Sample LS03 is from sandstones of the Lower Cambrian Qingxi Formation in the Longsheng area (Fig. 2e). A total of 76 concordant ages (Fig. 4) range from 3386 to 520 Ma. Ages mainly fall into five groups at 600–560 Ma, 1177–700 Ma, 1650–1278 Ma and 2668–2411 Ma. There are three isolated zircon ages at 660 Ma, 3018 Ma and 3386 Ma. The main range contains two sub-peaks at 799 and 977 Ma.

Sample LS04 was collected from sandstones of the Upper Cambrian Bianxi Formation in the Longsheng area (Fig. 2e). A total of 75 concordant ages range from 3776 to 529 Ma (Fig. 4). Ages mainly fall into five groups, with 607–529 Ma, 1131–777 Ma, 1677–1409 Ma, 2.5–2.4 Ga and 2.8–2.6 Ga. The main range occurs as three sub-peaks at *c.* 830 Ma, 960 Ma and 1098 Ma.

Sample LS07 is from Ordovician sandstone in the Huangai Formation exposed in the Longsheng area (Fig. 2e). A total of 77 concordant ages range from 2656 to 523 Ma (Fig. 4). Ages are mainly represented by two main groups at 580–523 Ma and 1100–780 Ma and several minor peaks at 1.4–1.2 Ga and 2.6–2.5 Ga.

5.a.3. Sandstone samples from southwest Hunan

Sample CB09 was obtained from the sandstones of the Silurian Tianlinkou Formation in the Chengbu area (Fig. 2e). Sixty-four concordant ages from this sample range from 2739 to 416 Ma (Fig. 4). Ages mainly fall into two groups at 440–416 Ma and 1128–770 Ma; others range from 2.7 to 1.2 Ga. Sample CB10 was collected from the Silurian Tianlinkou Formation in Chengbu (Fig. 2e). A total of 61 concordant ages (Fig. 4) were obtained that range from 2658 to 413 Ma. Two main groups at 457–413 Ma and 1225–719 Ma predominate and others range from 2.6 to 1.4 Ga.

5.b. Zircon Hf isotopes

Zircon Hf isotope compositions were analysed on 44 zircons from sample LS04 and 58 zircons from sample LS07. Hafnium isotope analytical data are presented in Table S2 in the online Supplementary Material at https://doi.org/10.1017/S0016756818000511. Zircons from these two samples exhibit overlapping ranges of $\varepsilon Hf(t)$ values (Fig. 5). The zircons with ages older than 700 Ma from both samples have similar broad $\varepsilon Hf(t)$ values ranging mainly from −13.7 to +5.6, except for several analyses that have values smaller than −17. The 654–524 Ma zircons in Ordovician sample LS07 have higher $\varepsilon Hf(t)$ values (−17.6 to +5.3) than the 566–529 Ma zircons in Cambrian sample LS04 (−19.3 to −10.4), except for one analysis in sample LS07 that has an $\varepsilon Hf(t)$ value of −25.7.

6. Discussion

6.a. Sources of detritus

The detrital zircon age spectra of three Precambrian samples (QD53, QD51 and LS01) share a common unimodal age distribution, with a dominant age range between 900 and 600 Ma, and lack ages older than 900 Ma. An additional sub-peak at 622–558 Ma is observed in sample QD51.

However, the features of the overlying Lower Palaeozoic samples (LS03, LS04, LS07, CB09 and CB10) differ from those of the underlying Upper Neoproterozoic samples. The Cambrian to Silurian samples display a common ‘multi-peak’ distribution pattern with age peaks at 600–520 Ma, 1100–780 Ma, 1.6–1.2 Ga and 2.8–2.5 Ga. An additional peak at 460–416 Ma is present in the Silurian samples (CB09 and CB10).

6.a.1. Provenance of the Cryogenian to Ediacaran samples

The magmatism accounting for the source of the Neoproterozoic detritus in the Cryogenian and Ediacaran samples with ages ranging from 900 to 700 Ma and

https://doi.org/10.1017/S0016756818000511 Published online by Cambridge University Press

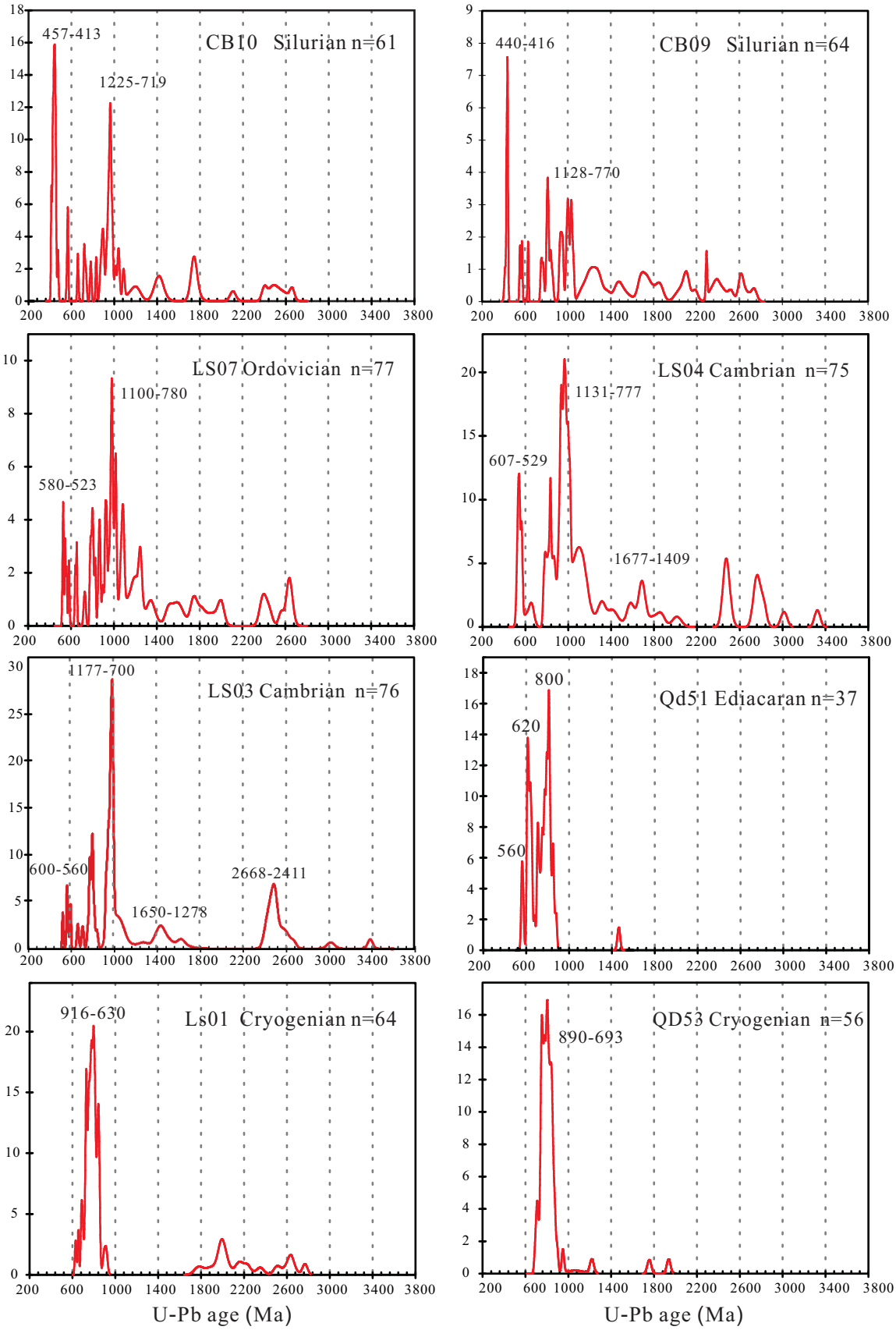

Figure 4. (Colour online) Relative probability density diagram of ages with concordance between 90 % and 110 % for the analysed samples.

https://doi.org/10.1017/S0016756818000511 Published online by Cambridge University Press

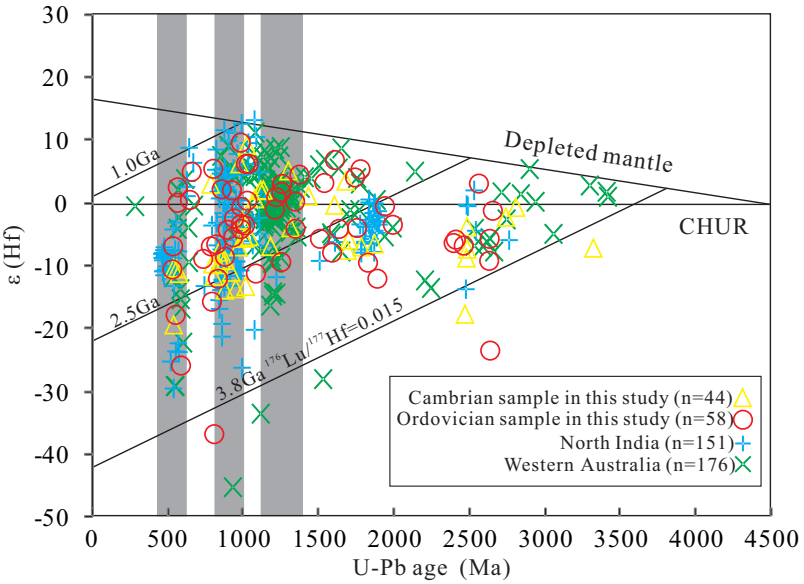

Figure 5. (Colour online) Plots of zircon εHf(*t*) values versus U–Pb ages of the detrital zircons from the Cambrian and Ordovician strata in this study. The detrital zircon from North India (Zhu *et al.* 2011; Spencer, Harris & Dorais, 2012) and West Australia (Veevers *et al.* 2005) are shown for comparison.

peaks around 820 and 880 Ma exists in the vicinity of the Jiangnan Orogenic belt adjacent to the study area. The collision of the Yangtze and Cathaysia Blocks along the Jiangnan Orogenic belt in the Mid-Neoproterozoic (1000 to 850 Ma) resulted in a widespread magmatic activity along a 1200 km long NEE-trending belt (Li *et al*. 2009; Zhou, Wang & Qiu, 2009; Charvet, 2013; Wang *et al*. 2014). Following this collision, the SE margin of the Yangtze Block underwent a regional-scale extension leading to the formation of a rift basin and emplacement of large volumes of 820–700 Ma mafic dykes (Li *et al*. 2002; Shu *et al.* 2011; Yao, Shu & Santosh, 2014; Cui *et al*. 2015; Lin *et al*. 2016). Therefore, the 820–700 Ma zircons in the detrital zircon age spectra of the Cryogenian to Ediacaran samples in this study are interpreted to have originated from 820–700 Ma syn-rift magmatism within the Nanhua rift basin. In addition, the 900–860 Ma syn-subduction and 860–820 syn-collisional magmatic rocks along the SE margin of the Yangtze Block provided material to the Cryogenian to Ediacaran sandstones.

Five zircon grains from sample LS01 are younger than 700 Ma, with ages between 698 and 630 Ma, and seven grains from sample QD51 have ages between 678 and 632 Ma, suggesting that the SE margin of the Yangtze also received detritus derived from the Upper Cryogenian magmatic rocks. The 700–630 Ma magmatism was associated with the opening of the Neoproterozoic Nanhua rift basin and has been documented in the N and NW margins of the Yangtze Block (Ling *et al*. 2008, 2010). The record of this magmatic activity, however, has rarely been recognized in the SE margin of the Yangtze Block. The 700–630 Ma detritus from Upper Neoproterozoic successions of the basin is inferred to have been sourced from a remnant of the oldland that was exposed synchronously with rifting along the NW Yangtze (Liu, Xu & Xu, 1995). Therefore, we suggest that the southward transportation of sediments might have been permitted from the NW to SE margins of the Yangtze Block.

The ten youngest zircons from the Ediacaran sample QD51 cluster within 622–558 Ma, with peaks at 560 Ma and 620 Ma. Although the distributions of 650–518 Ma tuff layers in the western segments of the Jiangnan Orogen indicate that the SCC was within the area affected by the Late Ediacaran to Early Cambrian volcanism (e.g. Jenkins, Cooper & Compston, 2002; Condon *et al*. 2005; Lan *et al*. 2015), the contemporaneous plutons that may represent potential sources are unknown in the SCC because they were either far away or are covered by the Lower Palaeozoic sedimentary rocks.

Conversely, the sources of the 630–550 Ma detritus have been previously interpreted to be exotic (Yu *et al.* 2008; Duan *et al*. 2011; Li, Li & Li, 2014; Chen *et al.* 2017). For example, they might be located either in the 600–500 Ma Prydz–Darling orogen along the west margin of Australia–Antarctica (Veevers *et al.* 2006; Veevers, 2007; Veevers & Saeed, 2011), or in the 650–550 Ma East African Orogen (Meert, 2003; Veevers, 2007; Robinson *et al.* 2014). Decelles *et al*. (2000) suggested that the 650–550 Ma East African Orogen provided the Neoproterozoic detritus to the Ediacaran basin where strata were deposited in the Nepal area of North India.

In order to best estimate the provenance of the 650–550 Ma zircons in the Upper Ediacaran strata presented in this study and other places in the SCC like Cathaysia (Yu *et al.* 2008, 2010; Xu *et al*. 2014*b*; W. H. Yao *et al*. 2014*b*, 2015) and the northern and western margins of the Yangtze (L. J. Wang *et al.*

https://doi.org/10.1017/S0016756818000511 Published online by Cambridge University Press

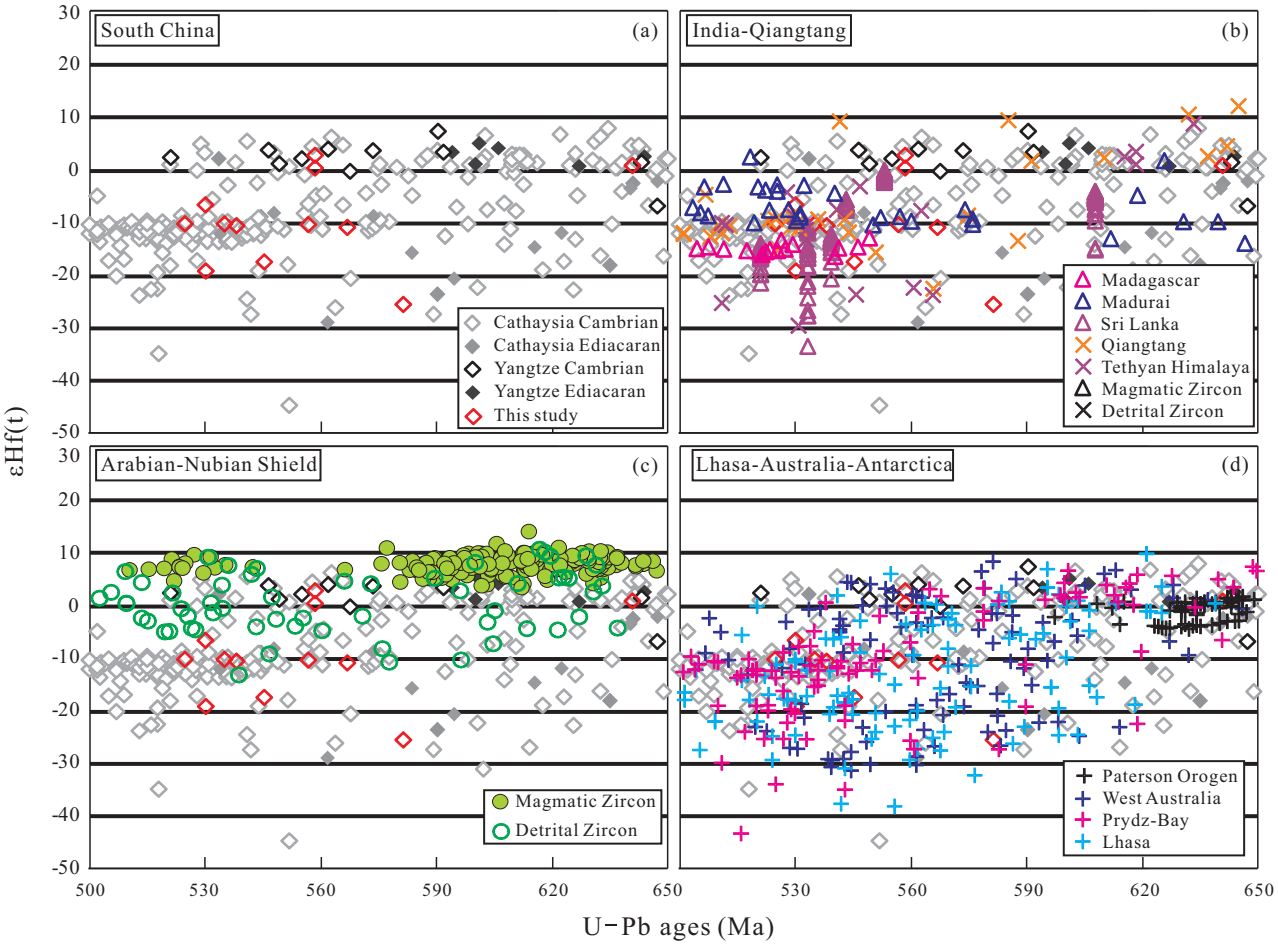

Figure 6. (Colour online) U–Pb and εHf(*t*) data from: (a) South China; (b) India and Qiangtang; (c) Arabian–Nubian Shield; (d) Lhasa–Australia–Antarctica. Sources of data: (a) Cathaysia Cambrian (Xu *et al.* 2014*b*; W. H. Yao *et al.* 2014*b*, 2015); Cathaysia Ediacaran (Yu *et al.* 2008, 2009); Yangtze Cambrian (Chen *et al.* 2017); Yangtze Ediacaran (L. J. Wang *et al.* 2013); (b) Sri Lanka Santosh *et al.* (2014*b*); Qiangtang (Zhu *et al.* 2012); Tethyan Himalaya (Zhu *et al.* 2012); Madurai (Santosh *et al.* 2017); Madagascar (Zhou *et al.* 2015); (c) Arabian–Nubian Shield (Robinson *et al.* 2014; Moghadam *et al.* 2017); (d) West Australia (Veevers *et al.* 2005; Martin, Collins & Kirkland, 2017); Paterson Orogen (Martin, Collins & Kirkland, 2017); Lhasa (Zhu *et al.* 2012); Prydz Bay (Veevers & Saeed, 2008).

2013; Chen *et al.* 2017), we plotted the εHf(*t*) values of these grains (Fig. 6) and compared them to those from several candidate potential source areas before reviewing their transporting capability. The εHf(*t*) values of 650–560 Ma in the Ediacaran strata in the northern and western margins of the Yangtze show positive values (+8 to +1); however, the contemporaneous detritus in the contemporary Cathaysia strata have a wider range of εHf(*t*) (+2 to −17) values. The εHf(*t*) values of the 650–560 Ma zircons in the rocks of northern and western Yangtze are comparable to those in the Late Neoproterozoic juvenile arc magmatic rocks in the Arabian–Nubian Shield as the northern extension of the East African Orogen (Robinson *et al.* 2014; Moghadam *et al.* 2017) and the Paterson Orogen in NW Australia (Martin, Collins & Kirkland, 2017). Considering that Australia was separated from the composite India–SCC in Ediacaran times (Xu *et al.* 2014*b*; Cawood *et al.* 2017), and the εHf(*t*) values of 650–560 Ma zircons in the Cathaysia section of the SCC are similar to those in the Upper Neoproterozoic magmatic rocks in South India, including Madurai (Santosh *et al.* 2017) and Sri Lanka Santosh *et al.* (2014*b*), we propose that the Late Ediacaran detritus in the SCC was mainly derived from the Arabia–India terrain rather than the India–Australia terrain.

The 650 to 550 Ma zircons only occupy a small portion of the total detrital age population in the Uppermost Neoproterozoic samples in our study area. Previous studies suggested that Uppermost Neoproterozoic sandstones were deposited in a failed intracontinental rift in the SE margin of the Yangtze in the Late Neoproterozoic (Wang & Li, 2003; Shu *et al.* 2014, 2015), indicating that it is very unlikely for SE Yangtze to receive detritus derived from the drainage system of Arabia across the ocean domain. However, Zhao *et al.* (2017) proposed an alternative model that the 650–600 Ma detritus was likely derived from volcanic arc ashes associated with Latest Neoproterozoic to Early Palaeozoic subduction along the northern margin of East Gondwana (L. J. Wang *et al.* 2013). Moreover, an extraordinary transport path from the East African

https://doi.org/10.1017/S0016756818000511 Published online by Cambridge University Press

Orogen and East Antarctica to the northern margin of India was proposed by Myrow *et al.* (2010), suggesting that they might have provided sediments to Cathaysia. On the basis of new zircon age and Hf isotope data, we hence propose that the 650–560 Ma zircons in the Ediacaran strata in the SCC were likely derived from the volcanic ashes from the Uppermost Neoproterozoic volcanic rocks in the northern extension of the East African Orogen and from the coeval magmatic rocks in South India.

6.a.2. Provenance of the Cambrian to Ordovician samples

The Cambrian to Ordovician samples have similar detrital zircon age spectra, but differ from those of the underlying strata, indicating a notable change in the provenance and transportation of detritus. The 1.1–0.9 Ga peak is notably absent from the Neoproterozoic samples, but is dominant in the Cambrian to Ordovician samples. Several 1.0–0.9 Ga ages have been reported from South China (Zhang *et al*. 2012; Y. J. Wang *et al*. 2013*d*; Li, Li & Li, 2014). The provenance of Upper Neoproterozoic to Ordovician samples from the SE margin of the SCC is therefore interpreted to be the uplifted Precambrian basement in the SCC, which suggests recycling of basement rocks (Wu *et al*. 2010; Li *et al*. 2013; Jiang *et al*. 2014).

However, evidence from palaeocurrent and palaeogeographic studies suggests that the provenance of detritus to the basin along the SE margin of the SCC in the Ediacaran and Cambrian is an Early Neoproterozoic orogenic belt outboard of the SCC, rather than the *c.* 1.0 Ga basement outcrops within Cathaysia that were submerged in the Late Neoproterozoic (Wang *et al*. 2010*b*; Xu *et al*. 2013; Yao, Li & Li, 2014*a*; W. H. Yao *et al*. 2014b). In current Gondwana reconstruction models, potential candidate orogens that may represent the source of this Early Neoproterozoic detritus include (1) the 990–900 Ma Rayner and Eastern Ghats belts (Fitzsimons, 2000; Boger, Wilson & Fanning, 2001) between India and Antarctica; (2) the 1.09–1.03 Ga Maud–Namaqua–Natal belts (Fitzsimons, 2000; Boger, Wilson & Fanning, 2001) between Africa and Antarctica; and (3) the 1.3–1.1 Ga Wilkes–Albany–Fraser belts (Cawood & Korsch, 2008; Ksienzyk *et al*. 2012) between West Australia and East Antarctica.

These Early Neoproterozoic belts in East Gondwana were cross-cut by several Latest Neoproterozoic to Early Cambrian orogenic belts (Fitzsimons, 2000; Cawood & Buchan, 2007; Zhu *et al*. 2012; Santosh *et al*. 2014*a*), including the 560−530 Ma Kuunga Orogen (Meert, 2003; Boger & Miller, 2004) and the 560−520 Ma Pinjarra Orogen (Fitzsimons, 2003; Veevers, 2004), both of which were associated with the internal convergence of East Gondwana, as well as the 550−470 Ma North India Orogen (Cawood, Johnson & Nemchin, 2007) and the 530−480 Ma Terra Australia Orogen (Cawood 2005; Cawood & Buchan, 2007). We prefer interpreting the 550–520 Ma detritus in the Cambrian to Ordovician samples to have been derived from exotic sources like the syn-orogenic detritus originated from the Latest Ediacaran to Cambrian Orogen within East Gondwana, because coeval magmatism is rarely reported in South China except for some sparse metamorphic ages between 530 and 490 Ma in Cathaysia (Zhang *et al.* 2011; Li *et al.* 2017). The uplifted basement rocks of the Early Neoproterozoic belts in East Gondwana hence were probably responsible for the input of the 1.1–0.9 Ga detritus in the SCC.

On the basis of comparisons of zircon age spectra (Fig. 7) and zircon εHf(*t*) values (Fig. 5), we suggest that the Cambrian to Ordovician samples share common provenance with the sandstones along the northern margin of East Gondwana, such as India. In addition, the 560−520 Ma grains in the Cambrian sample LS04 show restricted εHf(*t*) (−12 to −10) values, similar to those in the Cambrian to Ordovician strata in Cathaysia (Xu *et al*. 2014*b*; W. H. Yao *et al*. 2014*b*). These ages are similar to the age of the rocks in the Prydz Belt (Veevers & Saeed, 2008) and Lhasa (Zhu *et al.* 2012) along NW Australia–Antarctica, and Madagascar in South India (Zhou *et al.* 2015) that represent potential sources for the Early Cambrian grains in the SCC. The 650−560 Ma grains in the Cambrian strata in the SCC show a wide range of εHf(*t*) (−32 to +9) values, with most grains having positive εHf(*t*) (0 to +9) values; these grains are likely have been derived from the Paterson Orogen in Australia (Martin, Collins & Kirkland, 2017). In conclusion, we suggest that the Cambrian–Ordovician sedimentary rocks deposited along the SE Yangtze Block were predominantly derived from the Latest Neoproterozoic to Early Ordovician magmatic rocks in South India and West Australia.

6.a.3. Provenance of the Silurian samples

In the age spectra of the Silurian samples, the peaks older than 500 Ma are identical to those of the pre-Silurian samples, indicating that the provenance of detritus of those ages changed little since the Early Palaeozoic, or the provenance of the Silurian samples is mainly the recycled materials from the underlying strata. The 460−410 Ma orogeny (Y. J. Wang *et al.* 2010, 2013*a*) had begun by the time these strata were deposited, and the exposed Cambrian to Ordovician strata may therefore have been the source of the Silurian sedimentation in the basin along the SE margin of the SCC (Yao, Li & Li, 2014*a*; W. H. Yao *et al.* 2014*b*).

The only difference between the Silurian sample age spectra and those of the older samples is the distribution within the 460−410 Ma age range. This age interval coincides with the timing of the massive 440−390 Ma S-type granite and migmatites (Wang *et al*. 2010*b*; Y. J. Wang *et al*. 2013*a*; Zhang *et al*. 2015). Therefore, both syn- and post-orogenic magmatic activities supplied abundant materials to the

https://doi.org/10.1017/S0016756818000511 Published online by Cambridge University Press

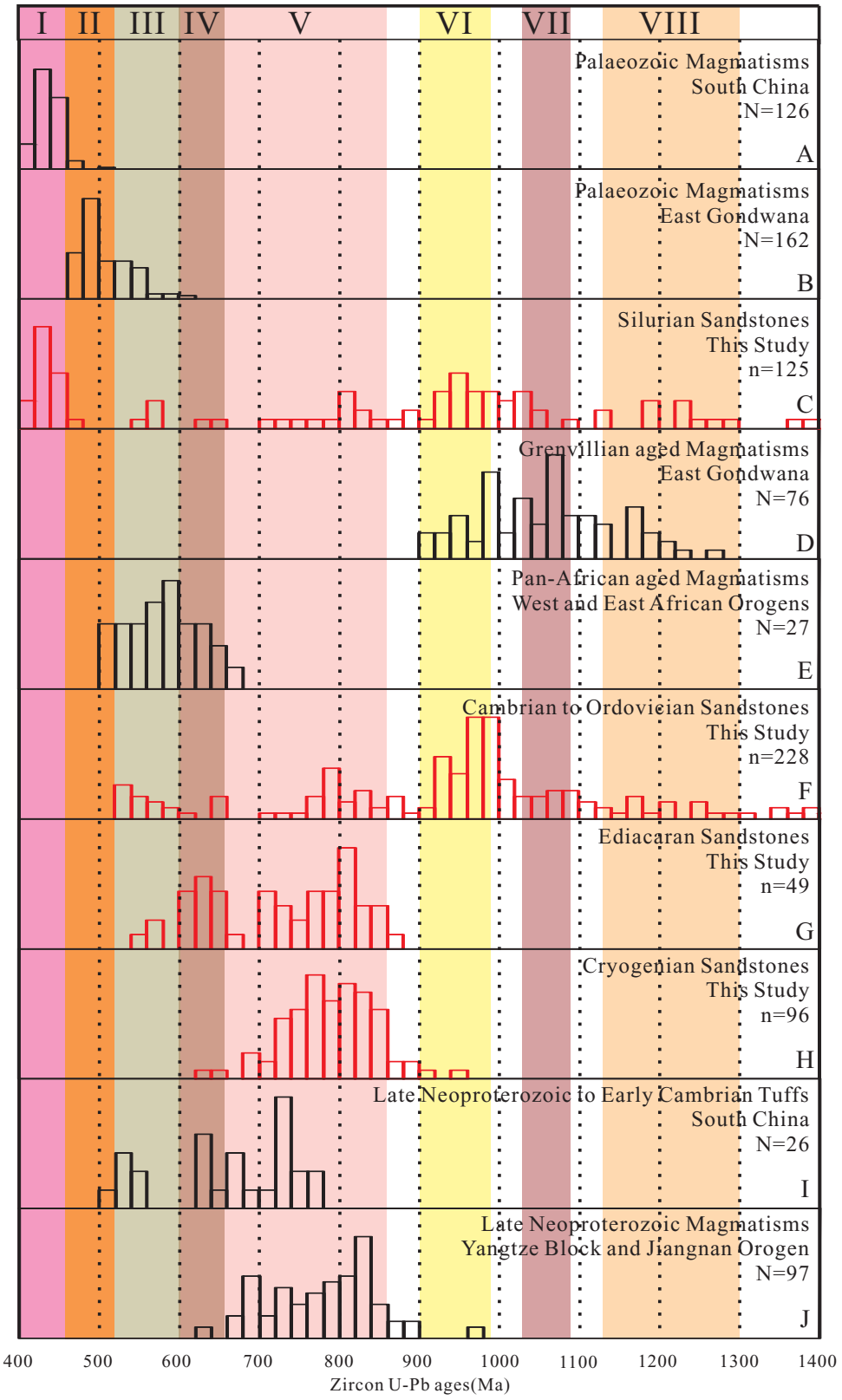

Figure 7. (Colour online) A summary of detrital zircon age distributions of samples from strata in the SCC and the potential sources. Sources of data: A – Y. J. Wang *et al.* 2013*d* and references therein; B – e.g. Goodge, Walker & Hansen, 1993; Y. J. Wang *et al.* 2013*b* and references therein; D – Fitzsimons, 2000 and references therein; E – Fitzsimons, 2000 and references therein; Valeriano *et al.* 2000; Neves *et al.* 2006, 2015; Silva *et al.* 2016; I – e.g. Jenkins, Cooper & Compston, 2002; Condon *et al.* 2005; J – e.g. Zhou, Wang & Qiu, 2009; Wang *et al.* 2014; the identical age clusters are divided as: I, the early Palaeozoic magmatisms in South China (460–400 Ma); II, the early Palaeozoic magmatisms along the north margin of East Gondwana (520–460 Ma); III, Pan-African aged events in Africa (650–500 Ma); IV, Brasiliano Orogeny in West Africa (630–600 Ma); V, Neoproterozoic magmatisms in SCC (900–680 Ma); VI, the Rayner – Eastern Ghats belts (990–900 Ma); VII, the Maud–Namaqua–Natal belts (1.09–1.03 Ga); VIII, the Wilkes–Albany–Fraser belts (1.3–1.1 Ga). *N* – number of samples; *n* – number of concordant zircon analyses.

https://doi.org/10.1017/S0016756818000511 Published online by Cambridge University Press

basin along the SE margin of the SCC. Additionally, the morphology of detrital zircons from the Silurian samples indicates multiple stages of recycling during sedimentation. The provenance of the Silurian sediments in the basin is inferred to include recycled pre-Silurian strata and an input of syn- and post-orogenic magmatic material from the intracontinental orogen of South China.

6.b. Provenance change of Cryogenian–Ordovician sediments in South China and its implications

The occurrence of the 622−558 Ma detritus in the sample QD51 from Upper Ediacaran reveals the first input from exotic sources into the SE Yangtze in the the Late Ediacaran. The change in provenance revealed in this contribution is represented by 550−520 Ma and 1.5−0.9 Ga detritus in the Cambrian samples. Moreover, the εHf(*t*) values of the 650−550 Ma zircons in the SCC indicate that coeval detritus was likely shed from the northern extension of the East African Orogen and interior of India in the Ediacaran. The εHf(*t*) values of 650−500 Ma zircons in the Cambrian sedimentary rocks of the SCC suggest additional possible source areas in NW Australia–Antarctica.

Based on our data and comparisons with the detrital zircon ages from the nearby continents, we propose a new model that places the SCC at the periphery of the NW margin of India in the Ediacaran, including the transportation of the detritus from India and Arabia to the SCC (Fig. 8). On the basis of tectono-stratigraphic correlations (Jiang, Sohl & Christie-Blick, 2003; W. H. Yao *et al*. 2014*b*), palaeontological similarities (Peng *et al*. 2009) and palaeomagnetic evidence (Li, Evans & Zhang, 2004; Zhang, 2004), previous studies proposed a link between India and the SCC as early as the Ediacaran. However, the distinct detrital zircon age spectra of the Ediacaran strata from Yangtze and East Gondwana contradict the link between these two areas (Fig. 8). An alternative explanation is that the Cathaysia side of the SCC was submerged (L. J. Wang *et al.* 2010; W. H. Yao *et al*. 2014*b*), and the depositional centre of the basin in the SE Yangtze Block had not migrated northward sufficiently by the Ediacaran (Yao & Li, 2016). Therefore, the Early Neoproterozoic detritus that was deposited in the Qiangtang, India and Cathaysia, was absent in the Yangtze Block in the Ediacaran. In contrast, the Ediacaran strata in the Yangtze Block were predominantly derived from the Middle to Late Neoproterozoic basement in the Yangtze and the Latest Neoproterozoic volcanic ashes from the Arabian–Nubian Shield (Fig. 6).

Previous Early Palaeozoic reconstruction models placed the SCC along the northern margins of Gondwana, with specific positions varying from the NW to NE margin of North India adjacent to Arabia or Australia, based on inconsistent faunal, palaeomagnetic and provenance explanations (Xu *et al*. 2014*b*; W. H. Yao *et al*. 2014*b*; Cawood *et al*. 2017; Chen *et al*. 2017; Wang *et al*. 2017). W. H. Yao *et al*. (2014*b*) proposed that the SCC collided with North India during Ediacaran to Ordovician times. This model was disputed for the lack of evidence to place the SCC as a downgoing plate for the inferred collision event (Cawood *et al*. 2017). Moreover, unconformity between the Cambrian and Ordovician strata in the Yunkai area along the southernmost margin of the SCC was observed (Wang *et al*. 2010*b*; Xu *et al*. 2013; Jiang *et al*. 2014), and two amphibolite–granulite facies metamorphic events on the Cathaysia side of the SCC at 533 Ma and 495 Ma were recently reported (Zhang *et al.* 2011; Li *et al*. 2017). These authors proposed that the Early Palaeozoic tectonic and metamorphic events in the SCC likely belong to the assembly of Australia and India–SCC during the Cambrian and Ordovician (Meert, 2003; Boger & Miller, 2004; Veevers, 2004).

As part of an ongoing debate on this region, new models have been proposed to explain the Early Palaeozoic ocean–continental configuration of the Gondwana proto-Tethyan margin, such as an archipelago ocean, an Andean-type active plate margin or a passive continental margin (Miller *et al*. 2001; Cawood, Johnson & Nemchin, 2007). In addition, Late Cambrian to Early Ordovician (510−480 Ma) granites occurring in the South Qiangtang were proposed to develop in the collision and post-collisional setting (Hu *et al.* 2015). These granites appear to be related to the accretion of other Asian microcontinental fragments (e.g. SCC), as the proto-Tethyan ocean subducted to the north margin of East Gondwana (Zhu *et al.* 2012).

However, the presence of a broad Cambrian ocean between the SCC and North India – South Qiangtang has been disputed on the basis of the following observations: (1) the absence of subduction- or collision-related magmatism in the Late Ediacaran to Ordovician strata in the SCC (e.g. Wang *et al.* 2010*b*; Shu *et al.* 2014); (2) the sedimentary facies across Cathaysia to Yangtze are continuous without records of Early Palaeozoic ophiolites in the SCC (e.g. Jiang *et al.* 2014; Yao, Li & Li, 2014*a*); and (3) the 1.1−0.9 Ga detritus derived from North India was able to reach the Cathaysia side of the SCC as early as the Ediacaran and to be transported northward to the Yangtze side of the SCC in the Cambrian. Accordingly, we propose a progressive filling of an intracontinental foreland basin between North India and Yangtze in the Cambrian, rather than an ocean–continental configuration process, to account for the transportation of detritus to Yangtze.

Based on our data, the input from Australia–Antarctica sources was observed in the Cambrian sedimentary strata in the SCC. Operation of a dextral strike-slip motion between the SCC and the North India margin during the Cambrian was proposed by Cocks & Torsvik (2013) to account for the contradictory faunal and palaeomagnetic link between the SCC and nearby continents in Ediacaran to Cambrian times. The mechanism for such a strike-slip motion, however, is still poorly constrained. The transportation of the 650−560 Ma detritus from the Paterson Orogen

https://doi.org/10.1017/S0016756818000511 Published online by Cambridge University Press

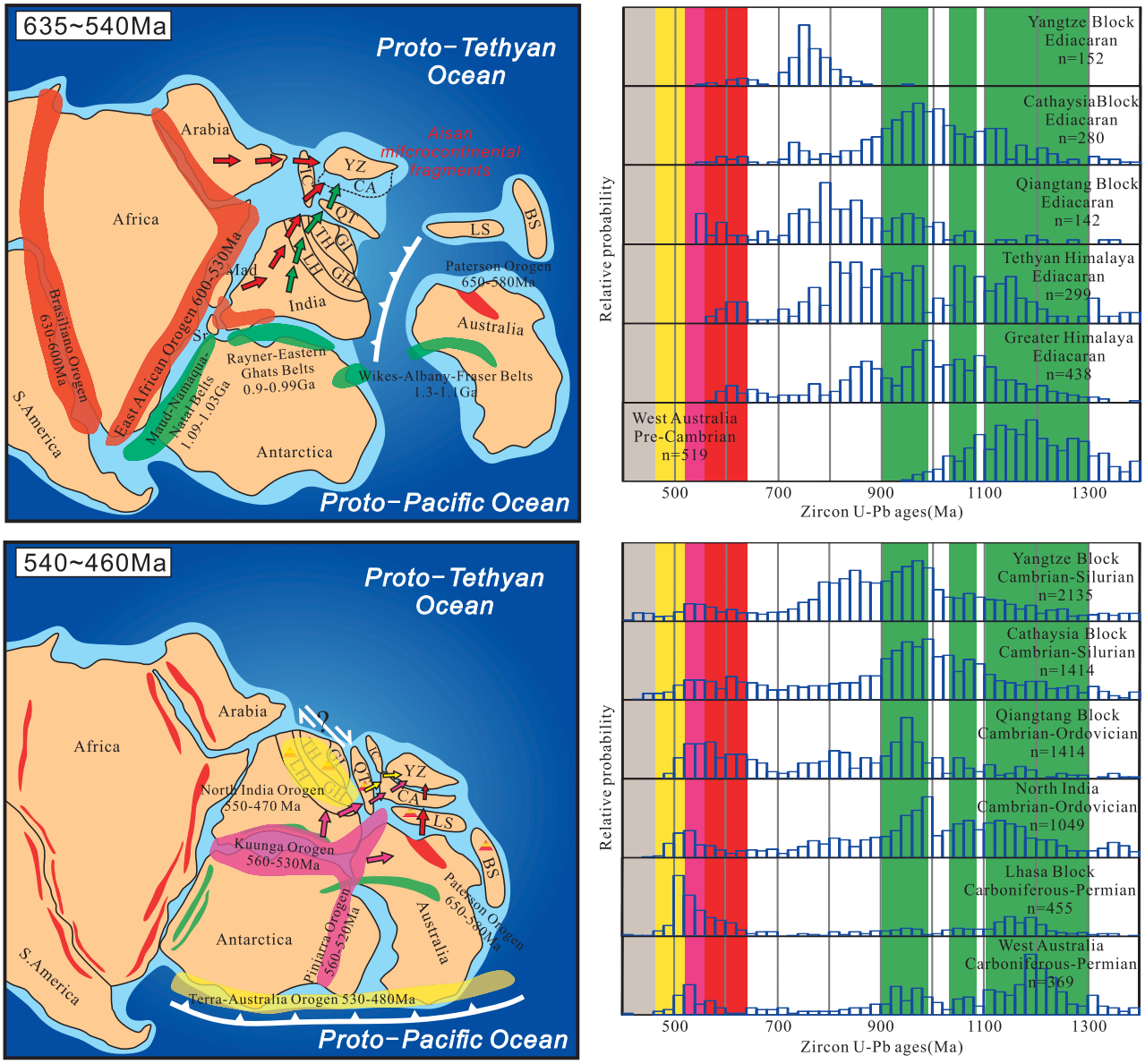

Figure 8. (Colour online) The model for the reconstruction of the Ediacaran to Silurian East Gondwana and the role of the SCC suggested by the regional comparison of detrital zircons among the Asian microcontinents fragments. Sources of data: 1, Yangtze Block: L. J. Wang *et al.* 2010; Hofmann *et al.* 2011; Xu *et al.* 2012, 2013; Li *et al.* 2013; Yao, Li & Li, 2014*a*; W. H. Yao *et al.* 2014*b*, 2015; Chen *et al.* 2016; 2, Cathaysia Block: Wan *et al.* 2007; Yu *et al.* 2009, 2010, 2012; L. J. Wang *et al.* 2010; Wu *et al.* 2010; Xu *et al.* 2014*b*; W. H. Yao *et al.* 2014*b*, 2015; Yu *et al.* 2014; 3, Qiangtang Block: Wang, Li & Chao, 2016; 4, Tethyan Himalaya: Webb, 2011; 5, Greater Himalaya: Martin *et al.* 2005; Gehrels *et al.* 2006, 2011; 6, West Australia: Ksienzyk *et al.* 2012; 7, North India (including the Cambrian to Ordovician samples from the Lesser, Tethyan and Greater Himalaya): Gehrels *et al.* 2006, 2011; Myrow *et al.* 2009, 2010; Hughes *et al.* 2011; Long *et al.* 2011; Webb, 2011; McQuarrie *et al.* 2013; 8, Lhasa Block: Gehrels *et al.* 2011; Zhu *et al.* 2011. *n* – number of concordant zircon analyses. QT – Qiangtang Block. IC– Indochina. LS – Lhasa Block. BS – Baoshan Block.YZ – Yangtze Block. CA – Cathaysia Block. Sr – Sri Lanka. Mad – Madagascar. TH – Tethyan Himalaya. GH – Great Himalaya. LH – Lesser Himalaya. GI – Great India.

in Australia (Martin, Collins & Kirkland, 2017) to the Cambrian basin in the southern margin of the SCC corresponds to the timing of the 560–520 Ma Pinjarra Orogen (Fitzsimons, 2003; Veevers, 2004) which led to the collision of Australia and India and the final assembly of East Gondwana (Santosh *et al.* 2014*a*). Thus, we suggest that the Australia–SCC link can explain the convergence between India and Australia, allowing the transportation of the 650–560 Ma detritus from the Paterson Orogen in NW Australia to the SCC.

7. Conclusions

1. Zircon age peaks in the Cryogenian and Ediacaran siliciclastic sedimentary rocks in the South China Craton (SCC) suggest that they are derived predominantly from 900–700 Ma proximal magmatic rocks in the block. The 662–558 Ma ages, however, indicate that the SE margin of Yangtze experienced arc volcanism along the north margin of East Gondwana in the Neoproterozoic, suggesting a spatial link between

https://doi.org/10.1017/S0016756818000511 Published online by Cambridge University Press

the SCC and East Gondwana as early as the Late Ediacaran.

2. The Cambrian to Ordovician siliciclastic sedimentary rocks display zircon age populations between 1.1and 0.9 Ga and between 600 and 500 Ma that are strikingly different from those revealed by the underlying strata. The εHf(*t*) values in these zircon grains are similar to those in the Prydz Belt, Lhasa and Madagascar. Northwestern Australia–Antarctica and India were the main source areas of the Cambrian siliciclastic sedimentary rocks in the SCC. The source area appears to have switched from NW India to NE India in the Cambrian, suggesting the SCC was affected by the intracontinental subduction between South China and South Qiangtang, and the assembly of India and Australia.

3. The Silurian siliciclastic sedimentary rocks display similar age peaks to the underlying strata except for 460−410 Ma detrital zircon ages, indicating inputs from the syn-orogenic sources from the Early Palaeozoic orogeny of South China.

Acknowledgements. The Chinese Geology Survey (Grant No. 12120114016701) and the National Natural Science Foundation of China (Grant No. 41472190) are gratefully acknowledged for funding for this study. Ali Polat acknowledges the support of China University of Geosciences at Wuhan and the Natural Sciences and Engineering Research Council of Canada (NSERC). We also acknowledge Prof. Yongsheng Liu for his assistance in the LA-ICP-MS U–Pb zircon analysis conducted at the State Key Laboratory of Geological Processes and Mineral Resources, China University of Geosciences, Wuhan. Prof. P. A. Cawood, Prof. J. Charvet, Prof. M. Faure and Prof. Liangshu Shu are thanked for their constructive comments which greatly helped improve the manuscript.

Supplementary material

To view supplementary material for this article, please visit https://doi.org/10.1017/S0016756818000511

References

BGMRGXP (Bureau of Geology and Mineral Resources of Guangxi Province). 1985. *Regional Geology of the Guangxi Province*. Beijing: Geological Publishing House, 243–256 pp. (in Chinese with English abstract).

BGMRHNP (Bureau of Geology and Mineral Resources of Hunan Province). 1988. *Regional Geology of the Hunan Province*. Beijing: Geological Publishing House, 121–157 pp. (in Chinese with English abstract).

Blichert-Toft, J., Chauvel, C. & Albarede, F. 1997. Separation of Hf and Lu for high-precision isotope analysis of rock samples by magnetic sector-multiple collector ICP-MS. *Contributions to Mineralogy and Petrology* **127**, 248–60.

Boger, S. D. & Miller, J. M. 2004. Terminal suturing of Gondwana and the onset of the Ross–Delamerian Orogeny: the cause and effect of an Early Cambrian reconfiguration of plate motions. *Earth and Planetary Science Letters* **219**, 35–48.

Boger, S. D., Wilson, C. J. L. & Fanning, C. M. 2001. Early Paleozoic tectonism within the East Antarctic craton: the final suture between east and west Gondwana? *Geology* **29**, 463–6.

BRMRGZP (Bureau of Geology and Mineral Resources of Guizhou Province). 1987. *Regional Geology of the Guizhou Province*. Beijing: Geological Publishing House, 156–167 pp. (in Chinese with English abstract).

Burrett, C., Zaw, K., Meffre, S., Lai, C. K., Khositanont, S., Chaodumrong, P., Udchachon, M., Ekins, S. & Halpin, J. 2014. The configuration of Greater Gondwana: evidence from LA ICPMS, U-Pb geochronology of detrital zircons from the Palaeozoic and Mesozoic of Southeast Asia and China. *Gondwana Research* **26**, 31–51.

Cawood, P. A. 2005. Terra Australis Orogen: Rodinia breakup and development of the Pacific and Iapetus margins of Gondwana during the Neoproterozoic and Paleozoic. *Earth-Science Reviews* **69**, 249–79.

Cawood, P. A. & Buchan, C. 2007. Linking accretionary orogenesis with supercontinent assembly. *Earth-Science Reviews* **82**, 217–56.

Cawood, P. A., Johnson, M. R. W. & Nemchin, A. A. 2007. Early Palaeozoic orogenesis along the Indian margin of Gondwana: tectonic response to Gondwana assembly. *Earth and Planetary Science Letters* **255**, 70–84.

Cawood, P. A. & Korsch, R. J. 2008. Assembling Australia: Proterozoic building of a continent. *Precambrian Research* **166**, 1–35.

Cawood, P. A., Wang, Y., Xu, Y. & Zhao, G. 2013. Locating South China in Rodinia and Gondwana: a fragment of Greater India lithosphere? *Geology* **41**, 903–6.

Cawood, P. A., Zhao, G. C., Yao, J. L., Wang, W., Xu, Y. J. & Wang, Y. J. 2017. Reconstructing South China in Phanerozoic and Precambrian supercontinents. *Earth-Science Reviews*. doi: 10.1016/j.earscirev.2017.06.001.

Charvet, J. 2013. The Neoproterozoic–Early Paleozoic tectonic evolution of the South China Block: an overview. *Journal of Asian Earth Sciences* **74**, 198–209.

Charvet, J., Shu, L. S., Faure, M., Choulet, F., Wang, B., Lu, H. F. & Le Breton, N. 2010. Structural development of the Lower Paleozoic belt of South China: genesis of an intracontinental orogen. *Journal of Asian Earth Sciences* **39**, 309–30.

Charvet, J., Shu, L. S., Shi, Y. S., Guo, L. Z. & Faure, M. 1996. The building of south China: collision of Yangzi and Cathaysia blocks, problems and tentative answers. *Journal of Southeast Asian Earth Sciences* **13**, 223–35.

Chen, Q., Sun, M., Long, X., Zhao, G., Wang, J., Yu, Y. & Yuan, C. 2017. Provenance study for the Paleozoic sedimentary rocks from the west Yangtze Block: constraint on possible link of South China to the Gondwana supercontinent reconstruction. *Precambrian Research* **309**, 271–89.

Chen, Q., Sun, M., Long, X. P., Zhao, G. C. & Yuan, C. 2016. U–Pb ages and Hf isotopic record of zircons from the late Neoproterozoic and Silurian–Devonian sedimentary rocks of the western Yangtze Block: implications for its tectonic evolution and continental affinity. *Gondwana Research* **31**, 184–99.

Cocks, L. R. M. & Torsvik, T. H. 2013. The dynamic evolution of the Palaeozoic geography of eastern Asia. *Earth-Science Reviews* **117**, 40–79.

Condon, D., Zhu, M. Y., Bowring, S., Wang, W., Yang, A. H. & Jin, Y. G. 2005. U-Pb ages from the neoproterozoic Doushantuo Formation, China. *Science* **308**, 95–8.

Cui, X. Z., Jiang, X. S., Wang, J., Wang, X. C., Zhuo, J. W., Deng, Q., Liao, S. Y., Wu, H., Jiang, Z. F. & Wei, Y. N. 2015. Mid-Neoproterozoic diabase dykes from Xide in the western Yangtze Block, South China: new evidence for continental rifting related to the breakup of Rodinia supercontinent. *Precambrian Research* **268**, 339–56.

Decelles, P. G., Gehrels, G. E., Quade, J., Lareau, B. & Spurlin, M. 2000. Tectonic implications of U-Pb zircon ages of the Himalayan Orogenic Belt in Nepal. *Science* **288**, 497–9.

Du, Q. D., Wang, Z. J., Wang, J., Qiu, Y. S., Jiang, X. S., Deng, Q. & Yang, F. 2013. Geochronology and paleoenvironment of the pre-Sturtian glacial strata: evidence from the Liantuo Formation in the Nanhua rift basin of the Yangtze Block, South China. *Precambrian Research* **233**, 118–31.

Duan, L., Meng, Q. R., Zhang, C. L. & Liu, X. M. 2011. Tracing the position of the South China block in Gondwana: U–Pb ages and Hf isotopes of Devonian detrital zircons. *Gondwana Research* **19**, 141–9.

Faure, M., Shu, L. S., Wang, B., Charvet, J., Choulet, F. & Monie, P. 2009. Intracontinental subduction: a possible mechanism for the Early Palaeozoic Orogen of SE China. *Terra Nova* **21**, 360–8.

Fitzsimons, I. C. W. 2000. Grenville-age basement provinces in East Antarctica: evidence for three separate collisional orogens. *Geology* **28**, 879–82.

Fitzsimons, I. C. W. 2003. Proterozoic basement provinces of southern and southwestern Australia, and their correlation with Antarctica. In *Proterozoic East Gondwana: Supercontinent Assembly and Breakup* (eds M. Yoshida, B. R. Windley & M. Yoshida), pp. 93–130. Geological Society of London, Special Publication no. 206.

Gao, S., Yang, J., Zhou, L., Li, M., Hu, Z. C., Guo, J. L., Yuan, H. L., Gong, H. J., Xiao, G. Q. & Wei, J. Q. 2011. Age and growth of the Archean Kongling terrain, South China, with emphasis on 3.3 Ga granitoid gneisses. *American Journal of Science* **311**, 153–82.

Gehrels, G. E., Decelles, P. G., Ojha, T. P. & Upreti, B. N. 2006. Geologic and U-Th-Pb geochronologic evidence for early Paleozoic tectonism in the Kathmandu thrust sheet, central Nepal Himalaya. *Geological Society of America Bulletin* **118**, 185–98.

Gehrels, G., Kapp, P., Decelles, P., Pullen, A., Blakey, R., Weislogel, A., Ding, L., Guynn, J., Martin, A. & Mcquarrie, N. 2011. Detrital zircon geochronology of pre-Tertiary strata in the Tibetan-Himalayan orogen. *Tectonics* **30**(5), TC5016. doi: 10.1029/2011TC002868.

Goodge, J. W., Walker, N. W. & Hansen, V. L. 1993. Neoproterozoic-Cambrian basement-involved orogenesis within the Antarctic margin of Gondwana. *Geology* **21**, 37–40.

Greentree, M. R., Li, Z. X., Li, X. H. & Wu, H. C. 2006. Late Mesoproterozoic to earliest Neoproterozoic basin record of the Sibao orogenesis in western South China and relationship to the assembly of Rodinia. *Precambrian Research* **151**, 79–100.

Hofmann, M., Linnemann, U., Rai, V., Becker, S., Gärtner, A. & Sagawe, A. 2011. The India and South China cratons at the margin of Rodinia – synchronous Neoproterozoic magmatism revealed by LA-ICP-MS zircon analyses. *Lithos* **123**, 176–87.

Hu, P. Y., Li, C., Wang, M., Xie, C. M. & Wu, Y. W. 2013. Cambrian volcanism in the Lhasa terrane, southern Tibet: record of an early Paleozoic Andean-type magmatic arc along the Gondwana proto-Tethyan margin. *Journal of Asian Earth Sciences* **77**, 91–107.

Hu, P. Y., Zhai, Q. G., Jahn, B. M., Wang, J., Li, C., Lee, H. Y. & Tang, S. H. 2015. Early Ordovician granites from the South Qiangtang terrane, northern Tibet: implications for the early Paleozoic tectonic evolution along the Gondwanan proto-Tethyan margin. *Lithos* **220–223**, 318–38.

Hu, Z. C., Gao, S., Liu, Y. S., Hu, S. H., Diekiterc, R. & Gunther, D. 2008. Signal enhancement in laser ablation ICP-MS by addition of nitrogen in the central channel gas. *Journal of Analytical Atomic Spectrometry* **23**, 1093–101.

Hu, Z. C., Liu, Y. S., Gao, S., Liu, W. G., Yang, L., Zhang, W., Ting, X. R., Lin, L., Zong, K. Q., Li, M., Chen, H. H. & Zhou, L. 2012a. Improved in situ Hf isotope ratio analysis of zircon using newly designed X skimmer cone and Jet sample cone in combination with the addition of nitrogen by laser ablation multiple collector ICP-MS. *Journal of Analytical Atomic Spectrometry* **27**, 1391–9.

Hu, Z. C., Liu, Y. S., Gao, S., Xiao, S. Q., Zhao, L. S., Gunther, D., Li, M., Zhang, W. & Zong, K. Q. 2012b. A 'wire' signal smoothing device for laser ablation inductively coupled plasma mass spectrometry analysis. *Spectrochimica Acta Part B: Atomic Spectroscopy* **78**, 50–7.

Hughes, N. C., Myrow, P. M., McKenzie, N. R., Harper, D. A. T., Bhargava, O. N., Tangri, S. K., Ghalley, K. S. & Fanning, C. M. 2011. Cambrian rocks and faunas of the Wachi La, Black Mountains, Bhutan. *Geological Magazine* **148**, 351–79.

Jenkins, R., Cooper, J. A. & Compston, W. 2002. Age and biostratigraphy of Early Cambrian tuffs from SE Australia and southern China. *Journal of the Geological Society* **159**, 645–58.

Jiang, B. Y., Sinclair, H. D., Niu, Y. X. & Yu, J. H. 2014. Late Neoproterozoic-Early Paleozoic evolution of the South China Block as a retroarc thrust wedge/foreland basin system. *International Journal of Earth Sciences* **103**, 23–40.

Jiang, G. Q., Sohl, L. E. & Christie-Blick, N. 2003. Neoproterozoic stratigraphic comparison of the Lesser Himalaya (India) and Yangtze block (south China): paleogeographic implications. *Geology* **31**, 917–20.

Jiao, W. F., Wu, Y. B., Yang, S. H., Peng, M. & Wang, J. 2009. The oldest basement rock in the Yangtze Craton revealed by zircon U-Pb age and Hf isotope composition. *Science in China Series D: Earth Sciences* **52**, 1393–9.

Ksienzyk, A. K., Jacobs, J., Boger, S. D., Košler, J., Sircombe, K. N. & Whitehouse, M. J. 2012. U–Pb ages of metamorphic monazite and detrital zircon from the Northampton Complex: evidence of two orogenic cycles in Western Australia. *Precambrian Research* **198**, 37–50.

Lan, Z. W., Li, X. H., Zhu, M. Y., Zhang, Q. R. & Li, Q. L. 2015. Revisiting the Liantuo Formation in Yangtze Block, South China: SIMS U–Pb zircon age constraints and regional and global significance. *Precambrian Research* **263**, 123–41.

Li, H. B., Jia, D., Wu, L., Zhang, Y., Yin, H. W., Wei, G. Q. & Li, B. L. 2013. Detrital zircon provenance of the Lower Yangtze foreland basin deposits: constraints on the evolution of the early Palaeozoic Wuyi–Yunkai orogenic belt in South China. *Geological Magazine* **150**, 959–74.

Li, L. M., Lin, S. F., Xing, G. F., Jiang, Y. & He, J. 2017. First direct evidence of Pan-African orogeny associated with Gondwana Assembly in the Cathaysia Block of Southern China. *Scientific Reports* **7**, 794.

Li, X. H., Li, W. X., Li, Z. X., Lo, C. H., Wang, J., Ye, M. F. & Yang, Y. H. 2009. Amalgamation between the Yangtze and Cathaysia Blocks in South China: constraints from SHRIMP U-Pb zircon ages, geochemistry and Nd-Hf isotopes of the Shuangxiwu volcanic rocks. *Precambrian Research* **174**, 117–28.

Li, X. H., Li, Z. X. & Li, W. X. 2014. Detrital zircon U–Pb age and Hf isotope constraints on the generation and reworking of Precambrian continental crust in the Cathaysia Block, South China: a synthesis. *Gondwana Research* **25**, 1202–15.

Li, Z. X., Evans, D. A. D. & Zhang, S. 2004. A 90° spin on Rodinia: possible causal links between the Neoproterozoic supercontinent, superplume, true polar wander and low-latitude glaciation. *Earth and Planetary Science Letters* **220**, 409–21.

Li, Z. X., Li, X. H., Li, W. X. & Ding, S. J. 2008. Was Cathaysia part of Proterozoic Laurentia? – new data from Hainan Island, south China. *Terra Nova* **20**, 154–64.

Li, Z. X., Li, X. H., Wartho, J. A., Clark, C., Li, W. X., Zhang, C. L. & Bao, C. 2010. Magmatic and metamorphic events during the early Paleozoic Wuyi-Yunkai orogeny, southeastern South China: new age constraints and pressure-temperature conditions. *Geological Society of America Bulletin* **122**, 772–93.

Li, Z. X., Li, X. H., Zhou, H. W. & Kinny, P. D. 2002. Grenvillian continental collision in south China: new SHRIMP U-Pb zircon results and implications for the configuration of Rodinia. *Geology* **30**, 163–6.

Li, Z. X., Zhang, L. H. & Powell, C. M. 1995. South China in Rodinia: part of the missing link between Australia–East Antarctica and Laurentia? *Geology* **23**, 407–10.

Lin, M. S., Peng, S. B., Jiang, X. F., Polat, A., Kusky, T., Wang, Q. & Deng, H. 2016. Geochemistry, petrogenesis and tectonic setting of Neoproterozoic mafic–ultramafic rocks from the western Jiangnan orogen, South China. *Gondwana Research* **35**, 338–56.

Ling, W. L., Duan, R. C., Liu, X. M., Cheng, J. P., Mao, X. W., Peng, L. H., Liu, Z. X., Yang, H. M. & Ren, B. F. 2010. U-Pb dating of detrital zircons from the Wudangshan Group in the South Qinling and its geological significance. *Chinese Science Bulletin* **55**, 2440–8.

Ling, W. L., Ren, B. F., Duan, R. C., Liu, X. M., Mao, X. W., Peng, L. H., Liu, Z. X., Cheng, J. P. & Yang, H. M. 2008. Timing of the Wudangshan, Yaolinghe volcanic sequences and mafic sills in South Qinling: U-Pb zircon geochronology and tectonic implication. *Chinese Science Bulletin* **53**, 2192–9.

Liu, B. J., Xu, X. S. & Xu, Q. 1995. Sequence stratigraphy and basin geodynamic of the southeastern margin of the Yangtze plate during the late Proterozoic to early Paleozoic. *Lithofacies Paleogeography* **5**, 1–16.

Liu, Y. S., Gao, S., Hu, Z. C., Gao, C. G., Zong, K. Q. & Wang, D. B. 2010. Continental and oceanic crust recycling-induced melt-peridotite interactions in the Trans-North China Orogen: U-Pb dating, Hf isotopes and trace elements in zircons of mantle xenoliths. *Journal of Petrology*, **51**, 537–71.

Liu, Y. S., Hu, Z. C., Gao, S., Gunther, D., Xu, J., Gao, C. G. & Chen, H. H. 2008. In situ analysis of major and trace elements of anhydrous minerals by LA-ICP-MS without applying an internal standard. *Chemical Geology* **257**, 34–43.

Long, S., McQuarrie, N., Tobgay, T., Rose, C., Gehrels, G. & Grujic, D. 2011. Tectonostratigraphy of the Lesser Himalaya of Bhutan: implications for the along-strike stratigraphic continuity of the northern Indian margin. *Geological Society of America Bulletin* **123**, 1406–26.

Ludwig, K. R. 2003. *ISOPLOT 3.00: A Geochronological Toolkit for Microsoft Excel*. Berkeley, California: Berkeley Geochronology Center, 39 pp.

Ma, X., Yang, K. G., Li, X. G., Dai, C. G., Zhang, H. & Zhou, Q. 2016. Neoproterozoic Jiangnan Orogeny in southeast Guizhou, South China: evidence from U–Pb ages for detrital zircons from the Sibao Group and Xiajiang Group. *Canadian Journal of Earth Sciences* **53**, 219–30.

Martin, A. J., Decelles, P. G., Gehrels, G. E., Patchett, P. J. & Isachsen, C. 2005. Isotopic and structural constraints on the location of the Main Central thrust in the Annapurna Range, central Nepal Himalaya. *Geological Society of America Bulletin* **117**, 926–44.

Martin, E. L., Collins, W. J. & Kirkland, C. L. 2017. An Australian source for Pacific-Gondwanan zircons: implications for the assembly of northeastern Gondwana. *Geology* **45**, 699–702.

McCulloch, M. T., Rosman, K. J. R. & De Laeter, J. R. 1977. The isotopic and elemental abundance of ytterbium in meteorites and terrestrial samples. *Geochimica et Cosmochimica Acta* **41**, 1703–7.

McQuarrie, N., Long, S. P., Tobgay, T., Nesbit, J. N., Gehrels, G. & Ducea, M. N. 2013. Documenting basin scale, geometry and provenance through detrital geochemical data: lessons from the Neoproterozoic to Ordovician Lesser, Greater, and Tethyan Himalayan strata of Bhutan. *Gondwana Research* **23**, 1491–510.

Meert, J. G. 2003. A synopsis of events related to the assembly of eastern Gondwana. *Tectonophysics* **362**, 1–40.

Miller, C., Thöni, M., Frank, W., Grasemann, B., Klötzli, U., Guntli, P. & Draganits, E. 2001. The early Palaeozoic magmatic event in the Northwest Himalaya, India: source, tectonic setting and age of emplacement. *Geological Magazine* **138**, 237–51.

Moghadam, H. S., Li, X., Griffin, W. L., Stern, R. J., Thomsen, T. B., Meinhold, G., Aharipour, R. & O'Reilly, S. Y. 2017. Early Paleozoic tectonic reconstruction of Iran: tales from detrital zircon geochronology. *Lithos* **268**, 87–101.

Murphy, J. B. & Nance, R. D. 1991. Supercontinent model for the contrasting character of Late Proterozoic orogenic belts. *Geology* **19**, 469–72.

Myrow, P. M., Hughes, N. C., Goodge, J. W., Fanning, C. M. & Williams, I. S. 2010. Extraordinary transport and mixing of sediment across Himalayan central Gondwana during the Cambrian-Ordovician. *Geological Society of America Bulletin* **122**, 1660–70.

Myrow, P. M., Hughes, N. C., Searle, M. P., Fanning, C. M., Peng, S. C. & Parcha, S. K. 2009. Stratigraphic correlation of Cambrian–Ordovician deposits along the Himalaya: implications for the age and nature of rocks in the Mount Everest region. *Geological Society of America Bulletin* **121**, 323–32.

Neves, S. P., Bruguier, O., Da Silva, J. M. R., Mariano, G., Da Silva Filho, A. F. & Teixeira, C. M. L. 2015. From extension to shortening: dating the onset of the

https://doi.org/10.1017/S0016756818000511 Published online by Cambridge University Press

Brasiliano Orogeny in eastern Borborema Province (NE Brazil). *Journal of South American Earth Sciences* **58**, 238–56.

Neves, S. P., Bruguier, O., Vauchez, A., Bosch, D., Da Silva, J. M. R. & Mariano, G. 2006. Timing of crust formation, deposition of supracrustal sequences, and Transamazonian and Brasiliano metamorphism in the East Pernambuco belt (Borborema Province, NE Brazil): implications for western Gondwana assembly. *Precambrian Research* **149**, 197–216.

Peng, S. C., Hughes, N. C., Heim, N. A., Sell, B. K., Zhu, X. J., Myrow, P. M. & Parcha, S. K. 2009. Cambrian trilobites from the Parahio and Zanskar valleys, Indian Himalaya. *Journal of Paleontology* **83**, 1–95.

Qiu, Y. M., Gao, S., McNaughton, N. J., Groves, D. I. & Ling, W. 2000. First evidence of >3.2 Ga continental crust in the Yangtze craton of south China and its implications for Archean crustal evolution and Phanerozoic tectonics. *Geology* **28**, 11–14.

Robinson, F. A., Foden, J. D., Collins, A. S. & Payne, J. L. 2014. Arabian Shield magmatic cycles and their relationship with Gondwana assembly: insights from zircon U–Pb and Hf isotopes. *Earth and Planetary Science Letters* **408**, 207–25.

Santosh, M., Hu, C., He, X., Li, S., Tsunogae, T., Shaji, E. & Indu, G. 2017. Neoproterozoic arc magmatism in the southern Madurai Block, India: subduction, relamination, continental outbuilding, and the growth of Gondwana. *Gondwana Research* **45**, 1–42.

Santosh, M., Maruyama, S., Sawaki, Y. & Meert, J. G. 2014a. The Cambrian Explosion: plume-driven birth of the second ecosystem on Earth. *Gondwana Research* **25**, 945–65.

Santosh, M., Tsunogae, T., Malaviarachchi, S. P. K., Zhang, Z., Ding, H., Tang, L. & Dharmapriya, P. L. 2014b. Neoproterozoic crustal evolution in Sri Lanka: insights from petrologic, geochemical and zircon U–Pb and Lu–Hf isotopic data and implications for Gondwana assembly. *Precambrian Research* **255**, 1–29.

Shu, L. S., Faure, M., Yu, J. H. & Jahn, B. M. 2011. Geochronological and geochemical features of the Cathaysia block (South China): new evidence for the Neoproterozoic breakup of Rodinia. *Precambrian Research* **187**, 263–76.

Shu, L. S., Jahn, B. M., Charvet, J., Santosh, M., Wang, B., Xu, X. S. & Jiang, S. Y. 2014. Early Paleozoic depositional environment and intraplate tectonomagmatism in the Cathaysia Block (South China): evidence from stratigraphic, structural, geochemical and geochronological investigations. *American Journal of Science* **314**, 154–86.

Shu, L. S., Wang, B., Cawood, P. A., Santosh, M. & Xu, Z. Q. 2015. Early Paleozoic and Early Mesozoic intraplate tectonic and magmatic events in the Cathaysia Block, South China. *Tectonics* **34**, 1600–21.

Silva, T. R., Ferreira, V. P., Lima, M. M. C. & Sial, A. N. 2016. Two stage mantle-derived granitic rocks and the onset of the Brasiliano orogeny: evidence from Sr, Nd, and O isotopes. *Lithos* **264**, 189–200.

Spencer, C. J., Harris, R. A. & Dorais, M. J. 2012. Depositional provenance of the Himalayan metamorphic core of Garhwal region, India: constrained by U–Pb and Hf isotopes in zircons. *Gondwana Research* **22**, 26–35.

Torsvik, T. H. & Cocks, L. R. M. 2009. The Lower Palaeozoic palaeogeographical evolution of the northeastern and eastern peri-Gondwanan margin from Turkey to New Zealand. In *Early Palaeozoic Peri-Gondwanan Terranes: Insights from Tectonics and Biogeography* (ed. M. G. Bassett), pp. 3–21. Geological Society of London, Special Publication no. 325.

Valeriano, C. D. M., Simões, L., Teixeira, W. & Heilbron, M. 2000. Southern Brasilia belt (SE Brazil): tectonic discontinuities, K–Ar data and evolution during the Neoproterozoic Brasiliano orogeny. *Revista Brasileira de Geociências* **30**, 195–9.

Veevers, J. J. 2004. Gondwanaland from 650–500 Ma assembly through 320 Ma merger in Pangea to 185–100 Ma breakup: supercontinental tectonics via stratigraphy and radiometric dating. *Earth-Science Reviews* **68**, 1–132.

Veevers, J. J. 2007. Pan-Gondwanaland post-collisional extension marked by 650–500 Ma alkaline rocks and carbonatites and related detrital zircons: a review. *Earth-Science Reviews* **83**, 1–47.

Veevers, J. J., Belousova, E. A., Saeed, A., Sircombe, K., Cooper, A. F. & Read, S. E. 2006. Pan-Gondwanaland detrital zircons from Australia analysed for Hf-isotopes and trace elements reflect an ice-covered Antarctic provenance of 700–500 Ma age, T DM of 2.0–1.0 Ga, and alkaline affinity. *Earth-Science Reviews* **76**, 135–74.

Veevers, J. J. & Saeed, A. 2008. Gamburtsev Subglacial Mountains provenance of Permian–Triassic sandstones in the Prince Charles Mountains and offshore Prydz Bay: integrated U–Pb and TDM ages and host-rock affinity from detrital zircons. *Gondwana Research* **14**, 316–42.

Veevers, J. J. & Saeed, A. 2011. Age and composition of Antarctic bedrock reflected by detrital zircons, erratics, and recycled microfossils in the Prydz Bay–Wilkes Land–Ross Sea–Marie Byrd Land sector (70–240° E). *Gondwana Research* **20**, 710–38.

Veevers, J. J., Saeed, A., Belousova, E. A. & Griffin, W. L. 2005. U–Pb ages and source composition by Hf-isotope and trace-element analysis of detrital zircons in Permian sandstone and modern sand from southwestern Australia and a review of the paleogeographical and denudational history of the Yilgarn Craton. *Earth Science Review* **68**, 245–79.

Wan, Y. S., Liu, D. Y., Xu, M. H., Zhuang, J. M., Song, B., Shi, Y. R. & Du, L. L. 2007. SHRIMP U–Pb zircon geochronology and geochemistry of metavolcanic and metasedimentary rocks in Northwestern Fujian, Cathaysia block, China: tectonic implications and the need to redefine lithostratigraphic units. *Gondwana Research* **12**, 166–83.

Wang, J. & Li, Z. X. 2003. History of Neoproterozoic rift basins in South China: implications for Rodinia breakup. *Precambrian Research* **122**, 141–58.

Wang, J., Zhou, X. L., Deng, Q., Fu, X. G., Duan, T. Z. & Guo, X. M. 2015. Sedimentary successions and the onset of the Neoproterozoic Jiangnan sub-basin in the Nanhua rift, South China. *International Journal of Earth Sciences* **104**, 521–39.

Wang, L. J., Griffin, W. L., Yu, J. H. & O'Reilly, S. Y. 2010. Precambrian crustal evolution of the Yangtze Block tracked by detrital zircons from Neoproterozoic sedimentary rocks. *Precambrian Research* **177**, 131–44.

Wang, L. J., Griffin, W. L., Yu, J. H. & O'Reilly, S. Y. 2013. U–Pb and Lu–Hf isotopes in detrital zircon from Neoproterozoic sedimentary rocks in the northern Yangtze Block: implications for Precambrian crustal evolution. *Gondwana Research* **23**, 1261–72.

Wang, L. J., Yu, J. H., Griffin, W. L. & O'Reilly, S. Y. 2012. Early crustal evolution in the western Yangtze Block: evidence from U-Pb and Lu-Hf isotopes on detrital zircons from sedimentary rocks. *Precambrian Research* **222**, 368–85.

Wang, M., Li, C. & Chao, M. X. 2016. Dating of detrital zircons from the Dabure clastic rocks: the discovery of Neoproterozoic strata in southern Qiangtang, Tibet. *International Geology Review* **58**, 216–27.

Wang, W., Zeng, M. F., Zhou, M. F., Zhao, J. H., Zheng, J. P. & Lan, Z. F. 2017. Age, provenance and tectonic setting of Neoproterozoic to early Paleozoic sequences in southeastern South China Block: constraints on its linkage to western Australia-East Antarctica. *Precambrian Research* **309**, 290–308.

Wang, W. & Zhou, M. F. 2012. Sedimentary records of the Yangtze Block (South China) and their correlation with equivalent Neoproterozoic sequences on adjacent continents. *Sedimentary Geology* **265**, 126–42.

Wang, W., Zhou, M. F., Yan, D. P., Li, L. & Malpas, J. 2013. Detrital zircon record of Neoproterozoic active-margin sedimentation in the eastern Jiangnan Orogen, South China. *Precambrian Research* **235**, 1–19.

Wang, X. L., Zhao, G. C., Zhou, J. C., Liu, Y. S. & Hu, J. 2008. Geochronology and Hf isotopes of zircon from volcanic rocks of the Shuangqiaoshan Group, South China: implications for the Neoproterozoic tectonic evolution of the eastern Jiangnan orogen. *Gondwana Research* **14**, 355–67.

Wang, X. L., Zhou, J. C., Griffin, W. L., Wang, R. C., Qiu, J. S., O Reilly, S. Y., Xu, X. S., Liu, X. M. & Zhang, G. L. 2007. Detrital zircon geochronology of Precambrian basement sequences in the Jiangnan orogen: dating the assembly of the Yangtze and Cathaysia Blocks. *Precambrian Research* **159**, 117–31.

Wang, X. L., Zhou, J. C., Griffin, W. L., Zhao, G. C., Yu, J. H., Qiu, J. S., Zhang, Y. J. & Xing, G. F. 2014. Geochemical zonation across a Neoproterozoic orogenic belt: isotopic evidence from granitoids and metasedimentary rocks of the Jiangnan orogen, China. *Precambrian Research* **242**, 154–71.

Wang, Y. J., Fan, W. M., Zhang, G. W. & Zhang, Y. H. 2013a. Phanerozoic tectonics of the South China Block: key observations and controversies. *Gondwana Research* **23**, 1273–305.

Wang, Y. J., Xing, X. W., Cawood, P. A., Lai, S. C., Xia, X. P., Fan, W. M., Liu, H. C. & Zhang, F. F. 2013b. Petrogenesis of early Paleozoic peraluminous granite in the Sibumasu Block of SW Yunnan and diachronous accretionary orogenesis along the northern margin of Gondwana. *Lithos* **182–183**, 67–85.

Wang, Y. J., Zhang, A. M., Cawood, P. A., Fan, W. M., Xu, J. F., Zhang, G. W. & Zhang, Y. Z. 2013c. Geochronological, geochemical and Nd–Hf–Os isotopic fingerprinting of an early Neoproterozoic arc–back-arc system in South China and its accretionary assembly along the margin of Rodinia. *Precambrian Research* **231**, 343–71.

Wang, Y. J., Zhang, A. M., Fan, W. M., Zhang, Y. H. & Zhang, Y. X. 2013d. Origin of paleosubduction-modified mantle for Silurian gabbro in the Cathaysia Block: geochronological and geochemical evidence. *Lithos* **160–161**, 37–54.

Wang, Y. J., Zhang, F. F., Fan, W. M., Zhang, G. W., Chen, S. Y., Cawood, P. A. & Zhang, A. M. 2010. Tectonic setting of the South China Block in the early Paleozoic: resolving intracontinental and ocean closure models from detrital zircon U-Pb geochronology. *Tectonics* **29**, TC6020. doi: 10.1029/TC002750.

Webb, A. A. 2011. Cenozoic tectonic history of the Himachal Himalaya (northwestern India) and its constraints on the formation mechanism of the Himalayan orogen. *Geosphere* **7**, 1013–61.

Wu, L., Jia, D., Li, H. B., Deng, F. & Li, Y. Q. 2010. Provenance of detrital zircons from the late Neoproterozoic to Ordovician sandstones of South China: implications for its continental affinity. *Geological Magazine* **147**, 974–80.

Xu, Y. J., Cawood, P. A., Du, Y. S., Hu, L. S., Yu, W. C., Zhu, Y. H. & Li, W. C. 2013. Linking south China to northern Australia and India on the margin of Gondwana: constraints from detrital zircon U-Pb and Hf isotopes in Cambrian strata. *Tectonics* **32**, 1547–58.

Xu, Y. J., Cawood, P. A., Du, Y. S., Huang, H. W. & Wang, X. Y. 2014a. Early Paleozoic orogenesis along Gondwana's northern margin constrained by provenance data from South China. *Tectonophysics* **636**, 40–51.

Xu, Y. J., Cawood, P. A., Du, Y. S., Zhong, Z. Q. & Hughes, N. C. 2014b. Terminal suturing of Gondwana along the southern margin of South China Craton: evidence from detrital zircon U-Pb ages and Hf isotopes in Cambrian and Ordovician strata, Hainan Island. *Tectonics* **33**, 2490–504.

Xu, Y. J., Du, Y. S., Cawood, P. A., Zhu, Y. H., Li, W. C. & Yu, W. C. 2012. Detrital zircon provenance of Upper Ordovician and Silurian strata in the northeastern Yangtze Block: response to orogenesis in South China. *Sedimentary Geology* **267–268**, 63–72.

Yao, J. L., Shu, L. S. & Santosh, M. 2014. Neoproterozoic arc-trench system and breakup of the South China Craton: constraints from N-MORB type and arc-related mafic rocks, and anorogenic granite in the Jiangnan orogenic belt. *Precambrian Research* **247**, 187–207.

Yao, W. H. & Li, Z. X. 2016. Tectonostratigraphic history of the Ediacaran–Silurian Nanhua foreland basin in South China. *Tectonophysics* **674**, 31–51.

Yao, W. H., Li, Z. X. & Li, W. X. 2014a. Was there a Cambrian ocean in South China? – Insight from detrital provenance analyses. *Geological Magazine* **152**, 184–91.

Yao, W. H., Li, Z. X., Li, W. X., Li, X. H. & Yang, J. H. 2014b. From Rodinia to Gondwanaland: a tale of detrital zircon provenance analyses from the southern Nanhua Basin, South China. *American Journal of Science* **314**, 278–313.

Yao, W. H., Li, Z. X., Li, W. X., Su, L. & Yang, J. H. 2015. Detrital provenance evolution of the Ediacaran–Silurian Nanhua foreland basin, South China. *Gondwana Research* **28**, 1449–65.

Yu, W. C., Du, Y. S., Cawood, P. A., Xu, Y. J. & Yang, J. H. 2014. Detrital zircon evidence for the reactivation of an Early Paleozoic syn-orogenic basin along the North Gondwana margin in South China. *Gondwana Research* **28**, 769–80.

Yu, J. H., O Reilly, S. Y., Wang, L. J., Griffin, W. L., Zhang, M., Wang, R. C., Jiang, S. Y. & Shu, L. S. 2008. Where was South China in the Rodinia supercontinent? *Precambrian Research* **164**, 1–15.

Yu, J. H., O Reilly, S. Y., Wang, L. J., Griffin, W. L., Zhou, M. F., Zhang, M. & Shu, L. S. 2010. Components and episodic growth of Precambrian crust in the Cathaysia Block, South China: evidence from U–Pb ages and Hf isotopes of zircons in Neoproterozoic sediments. *Precambrian Research* **181**, 97–114.

Yu, J. H., O Reilly, S. Y., Zhou, M. F., Griffin, W. L. & Wang, L. J. 2012. U–Pb geochronology and Hf–Nd isotopic geochemistry of the Badu Complex, Southeastern China: implications for the Precambrian crustal evolution and paleogeography of the Cathaysia Block. *Precambrian Research* **222**, 424–49.

Yu, J. H., Wang, L. J., O Reilly, S. Y., Griffin, W. L., Zhang, M., Li, C. Z. & Shu, L. S. 2009. A Paleoproterozoic orogeny recorded in a long-lived cratonic remnant (Wuyishan terrane), eastern Cathaysia Block, China. *Precambrian Research* **174**, 347–63.

Zhang, A. M., Wang, Y. J., Fan, W. M., Zhang, Y. Z. & Yang, J. 2012. Earliest Neoproterozoic (ca. 1.0Ga) arc–back-arc basin nature along the northern Yunkai Domain of the Cathaysia Block: geochronological and geochemical evidence from the metabasite. *Precambrian Research* **220–221**, 217–33.

Zhang, A. M., Wang, Y. J., Fan, W. M., Zhang, F. F. & Zhang, Y. Z. 2011. La-ICPMS Zircon U-Pb geochronology and Hf isotopic composition of the Taoxi Migmatite (Wuping): constraints on the formation age of the Taoxi Complex and the Yunanian Event. *Geotectonica et Metallogenia* **35**, 64–72 (in Chinese with English abstract).

Zhang, C. L., Santosh, M., Zhu, Q. B., Chen, X. Y. & Huang, W. C. 2015. The Gondwana connection of South China: evidence from monazite and zircon geochronology in the Cathaysia Block. *Gondwana Research* **28**, 1137–51.

Zhang, S. H. 2004. South China's Gondwana connection in the Paleozoic: paleomagnetic evidence. *Progress in Natural Science* **14**, 85–90.

Zhang, X. Z., Dong, Y. S., Li, C., Deng, M. R., Zhang, L. & Xu, W. 2014. Silurian high-pressure granulites from Central Qiangtang, Tibet: constraints on early Paleozoic collision along the northeastern margin of Gondwana. *Earth and Planetary Science Letters* **405**, 39–51.

Zhao, G. C. & Cawood, P. A. 1999. Tectonothermal evolution of the Mayuan assemblage in the Cathaysia Block: implications for neoproterozoic collision-related assembly of the South China craton. *American Journal of Science* **299**, 309–39.

Zhao, G. C. & Cawood, P. A. 2012. Precambrian geology of China. *Precambrian Research* **222**, 13–54.

Zhao, J. H., Zhou, M. F., Yan, D. P., Zheng, J. P. & Li, J. W. 2011. Reappraisal of the ages of Neoproterozoic strata in South China: no connection with the Grenvillian orogeny. *Geology* **39**, 299–302.

Zhao, T. Y., Feng, Q. L., Metcalfe, I., Milan, L. A., Liu, G. C., & Zhang, Z. B. 2017. Detrital zircon U-Pb-Hf isotopes and provenance of Late Neoproterozoic and Early Paleozoic sediments of the Simao and Baoshan blocks, SW China: implications for Proto-Tethys and Paleo-Tethys evolution and Gondwana reconstruction. *Gondwana Research* **51**, 193–208.

Zhao, X. F., Zhou, M. F., Li, J. W., Sun, M., Gao, J. F., Sun, W. H. & Yang, J. H. 2010. Late Paleoproterozoic to early Mesoproterozoic Dongchuan Group in Yunnan, SW China: implications for tectonic evolution of the Yangtze Block. *Precambrian Research* **182**, 57–69.

Zheng, J. P., Griffin, W. L., O'Reilly, S. Y., Zhang, M., Pearson, N. & Pan, Y. M. 2006. Widespread Archean basement beneath the Yangtze craton. *Geology* **34**, 417–20.

Zhou, J. C., Wang, X. L. & Qiu, J. S. 2009. Geochronology of Neoproterozoic mafic rocks and sandstones from northeastern Guizhou, South China: coeval arc magmatism and sedimentation. *Precambrian Research* **170**, 27–42.

Zhou, J. L., Rasoamalala, V., Razoeliarimalala, M., Ralison, B. & Luo, Z. H. 2015. Age and geochemistry of Early Cambrian post-collisional granites from the Ambatondrazaka area in east-central Madagascar. *Journal of African Earth Sciences* **106**, 75–86.

Zhu, D. C., Zhao, Z. D., Niu, Y., Dilek, Y. & Mo, X. X. 2011. Lhasa terrane in southern tibet came from Australia. *Geology* **39**, 727–730.

Zhu, D. C., Zhao, Z. D., Niu, Y. L., Dilek, Y., Wang, Q., Ji, W. H., Dong, G. C., Sui, Q. L., Liu, Y. S., Yuan, H. L. & Mo, X. X. 2012. Cambrian bimodal volcanism in the Lhasa Terrane, southern Tibet: record of an early Paleozoic Andean-type magmatic arc in the Australian proto-Tethyan margin. *Chemical Geology* **328**, 290–308.